Univerzita Karlova v Praze

Matematicko-fyzikální fakulta

BAKALÁŘSKÁ PRÁCE

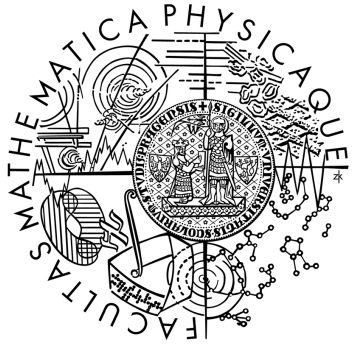

Lukáš Malina

Testování polovodičových detektorů typu DEPFET

Ústav částicové a jaderné fyziky

Vedoucí bakalářské práce: RNDr. Peter Kodyš, CSc.

Studijní program: Fyzika

Studijní obor: Obecná fyzika

Praha 2011

Charles University in Prague

Faculty of Mathematics and Physics

BACHELOR THESIS

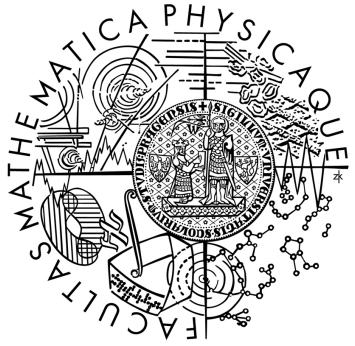

Lukáš Malina

Tests of DEPFET Semiconductor Detectors

Institute of Particle and Nuclear Physics

Supervisor: Peter Kodyš, PhD.

Study programme: Physics

Specialization: General physics

Prague 2011

I would like to thank all the people, who introduced me into problematics, especially to my supervisor Peter Kodyš and his coleague Zdeněk Doležal, for help with laser test setup and valuable discussions.

I declare that I carried out this bachelor thesis independently, and only with the cited sources, literature and other professional sources.

I understand that my work relates to the rights and obligations under the Act No. 121/2000 Coll., the Copyright Act, as amended, in particular the fact that the Charles University in Prague has the right to conclude a license agreement on the use of this work as a school work pursuant to Section 60 paragraph 1 of the Copyright Act.

In ..... date ..... Signature

Název práce: Testování polovodičových detektorů typu DEPFET

Autor: Lukáš Malina

Katedra: Ústav částicové a jaderné fyziky

Vedoucí bakalářské práce: RNDr. Peter Kodyš, CSc.

Abstrakt: Pixelové detektory typu DEPFET byly vynalezeny před více než dvaceti lety, od té doby jsou stále vyvíjeny, například pro japonský experiment Belle II. V této práci jsme zkoumali vlastnosti čtecího cyklu matice detektoru a posun vypočtených poloh zásahů u okrajů detektoru směrem dovnitř, tzv. okrajový efekt. Hlavním cílem této práce bylo seznámit se s detektory částic a jejich principy a speciálně s maticemi DEPFET, sestavit laserovou testovací aparaturu, napsat ovládací makro (ROOT) pro automatizaci měření, provést vlastní měření a analyzovat získaná data. Pro tyto účely jsme použili třínanosekundové červené laserové pulsy, stolky s pojezdy s velmi jemným krokem a dva pulsní generátory. Výsledkem práce je optimalizace napětí mezi vnější okruhem a vnitřkem aktivní oblasti detektoru, která zredukovala okrajový efekt circa na polovinu. Byly zjištěny časové vlastnosti detektoru, doba potřebná k odvedení náboje a čas během něhož se vyčítá matice detektoru.

Klíčová slova: laser test, ROOT, okrajový efekt, pixelový detektor, křemíkový polovodičový detektor

Title: Tests of DEPFET Semiconductor Detectors

Author: Lukáš Malina

Department: Institute of Particle and Nuclear Physics

Supervisor: Peter Kodyš, PhD.

Abstract: DEPFET pixel detectors were developed more than 20 years ago and they are still being improved, for example on Belle II experiment in Japan. In this thesis we studied the properties of readout cycle of detector matrix and the movement of counted hit positions close to the edges of DEPFET matrix, the which is reffered to as edge effect. The main goal of this work was to familiarize with particle detectors and their principles, especially with DEPFET matrices, to set up laser test system and to write ROOT macro for measurement automatization, run the measurement and analyze obtained data. For this purpose we used red 3 nanosecond long laser pulses, moving stages with very fine step and two connected pulse generators. As a result, the voltage between the outer ring and the inner part of the detector active area was optimalised, the edge effect was reduced by a factor of 2. The time properties of readout cycle, the time period of charge clearing and the time in which is the matrix read out, have been found.

Keywords: Laser Test, ROOT, Edge Effect, Pixel Detector, Silicon Semiconductor Detector

Contents

Introduction **2**

1 Detectors in HEP **3**

1.1 Colliding Beam Detector 3

1.2 Particle Interactions with Silicon 4

2 DEPFET **6**

2.1 Principle 6

2.2 Readout cycle 7

2.3 Construction 9

3 Laser Test **11**

3.1 Laser Test Setup 11

3.2 Software 13

3.2.1 ROOT macros for running the measurements 15

3.3 Measurement 16

3.4 Data Analysis 18

3.4.1 ROOT macros for analysis 23

4 Results **26**

4.1 Edge Effect 26

4.2 Time Properties 27

4.3 Comparison to Beam Test 31

5 Discussion **33**

Conclusions **35**

References **36**

List of Abbreviations **39**

Attachments **40**

Introduction

In High Energy Physics (HEP) experiments are usually implemented in two ways: accelerated charged particles interacting with particles in a fixed target or particles accelerated in opposite direction (colliders). Nowadays, accelerated particles have the energy in GeV or TeV range, their collisions can produce heavy or unstable particles, which dacay immediately into secondary particles. Many different parameter need to be determined for a complete reconstruction of an event, such as vertex position, decay path, angular distribution, momentum, energy etc. This cannot be measured by a single detector, wide range of detectors focusing on measurement of these needed quantities were developed. Systems composed of these sub-detectors are built to obtain enough quantities for complete event reconstruction. The progress in development of semicondutor detectors resulted in their wide usage for example as a position sensitive sensors. They are often used for tracking and vertexing (measurement of vertex positions), due to their high spatial resolution. In this thesis we tested DEPFET (DEPleted Field Effect Transistor) pixel semiconductor detectors by laser light.

Working on this thesis was a got introduction to the detection of particles and construction of detectors. An existing measurement system was used to set up the laser test. The measurement was conducted using already installed software packages for DAQ (Data AcQuisition) and power supply management, as well as TLU (Trigger Logic Unit) and DQM (Data Quality Monitor). For running the measurement ROOT macros `Timewindow.cpp`, `DepfetMatrixXY1.cpp` and `DepfetmatrixXY2.cpp` have been written. All these macros were inspired by a former macro `DepfetmatrixXY.cpp` provided in original setup. Functions `SetDEPFETPer` and `SetTrig` were added into existing macro `LTPK_GPIB.cpp`, they were strongly inspired by its function `SetDEPFET`. All the other macros for running the laser test were present in original setup as well. The first steps in data analysis, from raw data to the hit center of gravity, have been present in the software already. The remaining steps of analysis were the basic goals of this thesis. For this purpose the ROOT macro `LTAnal.cpp` was written. Results of this work were also published in [1].

1. Detectors in HEP

The detector concept can be based on every interaction process of particles and radiation, but no particles or radiation can be detected without any interaction. There are specific interactions for charged particles which are different from those of neutral particles. There are many of these processes. It causes development of plenty of detector types, even different processes may be relevant at different energies of particles. The main interactions of charged particles with matter are ionization, excitation, pair production and the bremsstrahlung energy losses. Neutral particles must interact with matter to produce charged particles which are then detected via their characteristic interaction processes. For example in the case of photons, these processes are the photoelectric effect, Compton scattering and electron-pozitron pair production. The electrons produced in these photon interactions can be observed through their ionisation in the sensitive volume of the detector. For the description of interactions mentioned above, see [2].
In section 1.1 the typical colliding beam detector is described. Interactions in silicon material are mentioned in the last section, especially of the visible light.

1.1 Colliding Beam Detector

In modern HEP experiments, the beam coliders are common, such as the LHC (Large Hadron Collider) [3] at CERN on Swiss-French border, or B Factory [4] at KEK in Japan. Particle beams are accelerated in several steps up to the energy in the range of GeV or TeV. There are two colliding beams, and the general-purpose detectors are built all around the interaction points, usually in cylindrical layers. Such a detector generally consists of (from inside out):

- The vertex detector is the position sensitive detector which contains usually several layers of semiconductor detectors. From the detected positions the tracks and their vertices are calculated, in order to minimise error it should be as close to interaction point as possible. It shold have minimal material budget to avoid multiple scattering. The other chalenge for vertex detectors is that the high accuracy (few units or tens of μm) is necessary.

- The tracking detector is used for the reconstruction of momentum of charged particles. It is done by positional sensitive measurement of curvature of a particle trajectory in a magnetic field. The necessity of minimal material budget is the same as in the case of vertex detector, it should minimise the multiple scattering and interactions of neutral particles. Good momentum resolution requires large (radius of 1 to 2 meters)[5] detectors in a strong magnetic field.

- The electromagnetic calorimeter measure the energy of electrons and photons. They create an electromagnetic shower in a material with high atomic number, the whole shower should be absorbed in the volume of calorimeter. A fine segmentation is required, due to necessity of matching the showers to the measured electron tracks.

- The energy of hadrons, which are passing through the electromagnetic calorimeter is measured in the hadronic calorimeter, which is usually made of iron due to its magnetic properties. The shower should be fully absorbed in the detector volume, the calorimeter should be large enough, the same as the electromagnetic one.

- In the last layer of collider detectors the muon are detected, for example by Drift Tubes (used in CMS [6] - Compact Muon Solenoid), which is filled by gas, and when the charged particle is passing through, it knocks the electron out of the atoms to the wire cathode.

The mentioned detector types do not necessarily make only one kind of measurement, for example segmented calorimeter can be used to determine particle tracks. However their primary purpose remains the same.

1.2 Particle Interactions with Silicon

Silicon is a semiconductor with a band gap of 1.1 eV. This means that photons with an energy bigger than the band gap can excite an electron from the valence to the conduction band. The absorption length of photons is shown as a function of the photon wavelength in Figure 1.1, it is from [5]. At wavelengths larger than

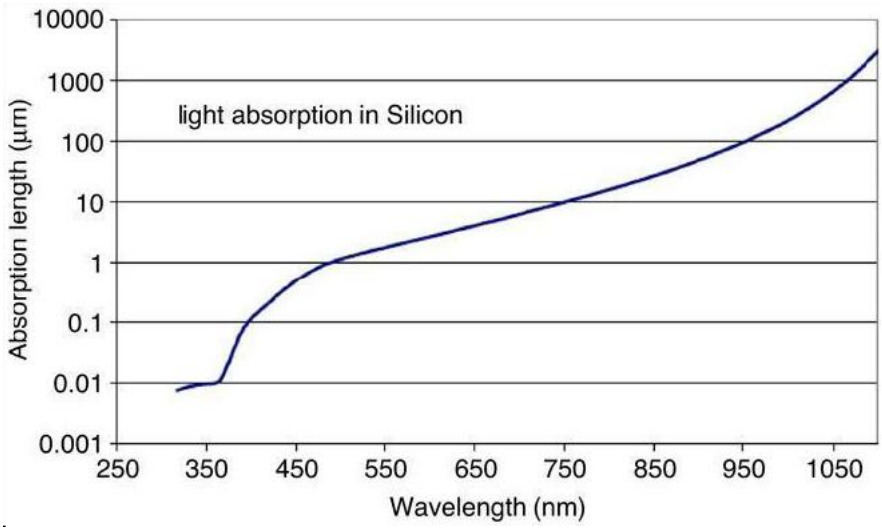

Figure 1.1: Photon attenuation length in silicon as function of the wavelength of the photon (at room temperature), from [5].

1100 nm silicon becomes transparent. Primarily there are three interactions of photons:

- Photoelectric effect - All the energy of photon can be measured.
- Compton scattering: Only a fraction of the photon energy is measured.
- Electron-pozitron pair creation.

On average an energy loss of about 3.6 eV is needed to generate one electron-hole pair, it is more than the energy of the band gap of 1.1 eV. The difference is a part of the energy losted in another processes. Charged particles ionize the silicon when passing through it, mean energy loss we get from Bethe-Bloch formula:

$$-\frac{\mathrm{d}E}{\mathrm{d}x} = \frac{4\pi}{m_e c^2} \cdot \frac{nz^2}{\beta^2} \cdot \left(\frac{e^2}{4\pi\varepsilon_0}\right) \cdot \left[\ln\left(\frac{2m_e c^2\beta^2}{I \cdot (1-\beta^2)}\right) - \beta^2 - \frac{\delta(\beta\gamma)}{2}\right] \tag{1.1}$$

, where $\beta = \frac{v}{c}$, v is velocity of the particle, E energy of the particle, x distance traveled by the particle, c speed of light ze is a particle charge, e is charge of electron, m_e is rest mass of the electron, n electron density of the target, I is mean excitation potential of the target and ϵ_0 vacuum permitivity and δ describes density effect corrections. Charged particles can knock the electrons in almost perpendicular direction. Such an electron (so called δ-electron) can create even more electron-hole pairs, than primary particle. This is badly influencing the spatial resolution.

2. DEPFET

The concept of DEPFET (DEPleted Field Effect Transistor) was proposed in 1987 by Kemmer and Lutz [7] and experimentally verified and successfully operated in 1990 [8]. The principle of the DEPFET is integration of MOSFET (Metal-Oxide-Semiconductor Field Effect Transistor) onto sidewards fully depleted n-doped silicon bulk. The major advantage is combination of detection and amplification. Nowadays DEPFET sensors are developed for two main purposes, the vertex detector for Belle II [9] and for future ILC (International Linear Colider) and X-ray imaging in astronomy.

2.1 Principle

The principle of DEPFET is shown in Figure 2.1 from [9]. A particle passing through the fully depleted n-Si bulk (from 50 μm to 450 μm thick) creates electron-hole pairs along its trajectory, electrical field inside a bulk then separate electrons from holes, which are attracted to p+ backplane with negative high voltage, used for depletion. In the meanwhile electrons are attracted to the internal gate underneath ($\approx 1\mu$m) the transistor channel, where they are accumulated. There is potential minimum for electrons made by additional n+ doping and because contacts on top side are biased with significantly smaller voltage than backplane. Signal charge stored in the internal gate effects the transistor channel current, the change is about 400 pA per electron in todays devices [10]. The collected electrons (as well as thermal electrons) can be removed from the internal gate by applying the positive voltage pulse to the clear contact. The deep p-well is beneath the clear contact to prevent signal charge from reaching the clear contact instead of the internal gate during the charge collection phase. P-well pasivate the clear contact during the collection time, although it always makes potential barrier. Very small capacitance of internal gate (due to much smaller dimensions in compare to sensitive volume) causes low noise performance of the sensor even at the room temperature. For the read out the voltage is applied to the external gate, switching on the transistor and the source-drain current is

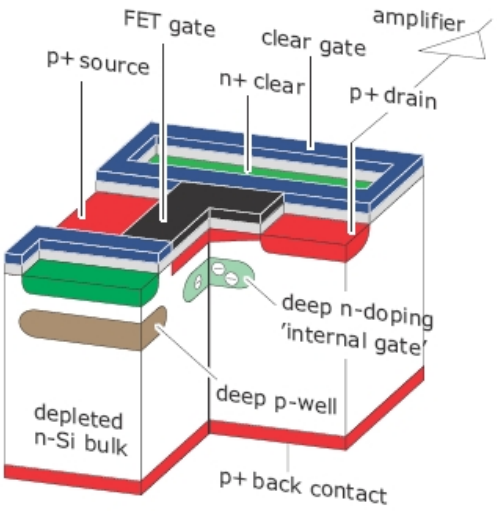

Figure 2.1: DEPFET pixel section: MOSFET transistor is integrated onto fully depleted n-Si bulk. The charge collected in internal gate influences the transistor current. Picture is from [9].

measured. This includes the other advantage of DEPFET detector which is low power consumption because the pixels are switched on only when they are read out. When they are switched off they need almost no power, but they are still sensitive.

2.2 Readout cycle

The readout cycle of individual DEPFET pixel is operated as follows[11]: The DEPFET is switched off, it is still sensitive to ionization and that's why electrons can be collected in internal gate. For read out the sensor a voltage is applied to the external gate, switching on the transistor. The source-drain current (which is changed by field of charge stored in internal gate) is then measured. After that is the positive voltage is applied to the clear contact to punch-through into the internal gate, which removes the electrons. The source-drain current is measured again (pedestal current defined by external gate voltage) and subtracted from the first reading, the difference corresponds to signal. Finally the transistor is switched off by seting back the external gate voltage.

DEPFET sensors can be operated collectively as an active pixel detector. In

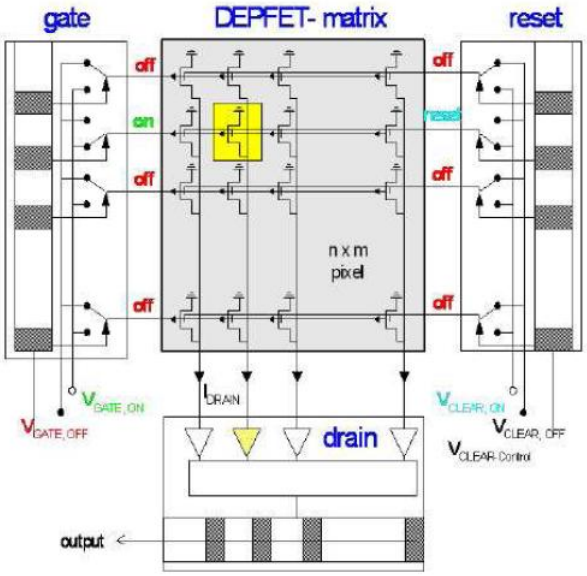

Figure 2.2: Scheme of DEPFET matrix operational principle, gates and clears are connected in row-like fashion to SWITCHER chips, drains are connected in column-like fashion to CURO chips. Scheme is from [9].

Figure 2.2 from [9] ilustrate the scheme of a DEPFET pixel matrix that is operated by Switcher chip, which is applying "on/off" voltage to the external gates, the so called "rolling shutter mode". When the row of DEPFET is on, source-drain currents are read by CURO (all at the same time) and they are stored there. Internal gates of all pixels in the selected row are then emptied by applying a positive pulse to the clear contacts in all pixels of selected row, after that their pedestal currents are measured and subtracted from the stored currents by the CURO readout chip. The difference between stored and pedestal current is proportional to charge collected in the internal gate. A measurement cycle consists of a collection phase (charge supporters are moving, especially electrons drift to the internal gate), the read out and the clearing of the internal gate. A pedestal subtraction is realized either by a consecutive Read-Clear-Read sequence (double sampling) or by a faster Read-Clear procedure (single sampling), where cached pedestal values are subtracted in the DHP (Data Handling Processor) readout chip.

This way, DEPFET matrix can work continuosly, it is cleared row by row and when the trigger comes, readout starts from the next row in rolling shutter mode.

A question rise up, what happens when hit comes too early or it comes too late according to the trigger? The expected scenario is when particle hit the detector and trigger comes after the clearing of whole matrix, no particle is detected, but when not the whole matrix is cleared when trigger comes, the probability of detecting the particle will be proportional to uncleared part of matrix as the starting row does not depend on position of hit. As the clearing time should be the same for all rows, a linear growing dependence of detection probability on hit delay is expected, when hit delay is negative. When hit and trigger are simultaneous the probability should equal to 1, considering only this effect. The similar situation becames when a particle passed through the detector after the trigger. As hit delay increases the probability of detection decreases again (it is proportional to unread out part of detector at the moment of hit) to zero, what happens in cases, when hit comes after the whole matrix has been read out. The probability is decresing in larger timescale than it was increasing, because there are more steps to do Read-Clear or even Read-Clear-Read instead of Clear. This effect is studied by measurement with different laser pulse delays according to the trigger.

2.3 Construction

During the years of development, there were several DEPFET matrix layouts, one of the newer ones developed for Belle II experiment in Japan is shown in Figure 2.3 from [12]. On the its left side is viewed the module with active area, Switcher3 chips by the right edge and CURO2 read out chips by bottom edge. In the top right corner is ilustrated a conection of Switchers. Very important is the picture on the right side in the middle, because there is visible the double pixel structure, there is only one Switcher gate contact and one clear contact per double row. On the other hand, there are two drains for one column, these facts together mean that one double row can be read out at once. In the cross section of the wafer is viewed the thinning, which is made for reduction of multiple scattering in detector material. Thinning has some limitations, because the collected charge is (roughly) proportional to sensor thickness, so when the sensor is thinned, the

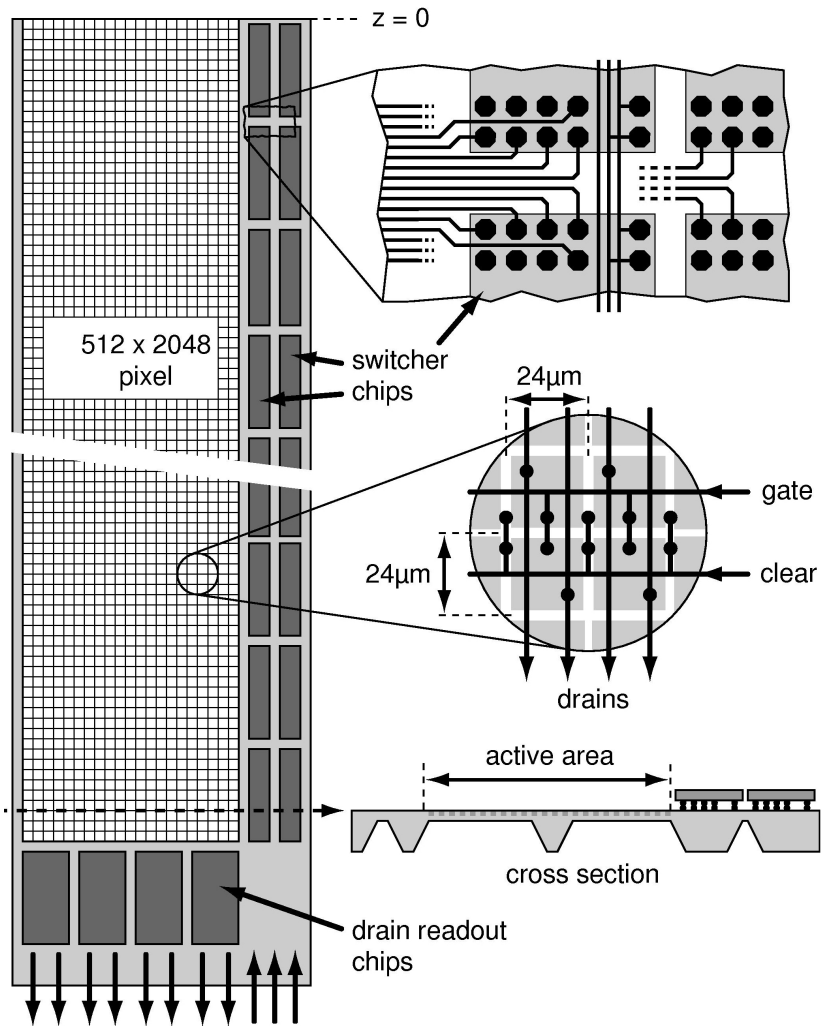

Figure 2.3: DEPFET Module developed for Belle II experiment, from [12].

signal is smaller and signal to noise ratio is also smaller.

In all the DEPFET beams were observed a systematic bias in the positional information reported by detectors, so called edge effect. The edge effect is a systematic shift of charge generated by particles in the detector bulk close to the border of active area. The effect comes from a potential difference between the active volume and the outter ring (Bulk Voltage), which is between 9 V and 10 V with respect to source. The edge effect is visible in distance up to 250 µm from borders. Ideally it would be expected, that edge effect may not be visible in the area farther from border than the dimensions of generated charge cloud in the bulk (several tens of µm) and that is why the edge effect was measured in this work. By changing the bulk voltage can be the electrical field more homogenous in the wafer plane.

3. Laser Test

In principal there are three ways of testing detectors. These are testing by beam, radioactive source (usually β - ray) or by laser. Beam tests are the closest to real usage in HEP experiments, but they are expensive. The problem of source tests is that there is small occupancy and the decays are stochastic. On the other hand, although laser tests aren't so close to reality, the laser is well defined, it give us the possibility hit the detector, where we want to and when we want to. There are differences between particles and light passing through the detector. When particles pass through δ-electrons can be produced and the electron-hole pairs are created along the whole particle paths (δ-electrons badly influence the spatial resolution).In case of laser testing, the electron-hole pairs are produced in whole volume where the light penetrates into Si-bulk. The other but not the last advantage of laser testing is the easier collection of huge statistics. We can measure the spatial and the time resolution more precisely than by the other ways, and that is why we chose laser testing. It should be said that laser tests have disadvantages to, there is need for a transparent backplane while testing by laser, the penetration depth increases with wavelength and the light can be reflected. Although the resolutions for photons, electrons, pions ... are entangled and similar, the given results are valid only for photons. In section 3.1 the laser testing setup is described. Section 3.2 describes software, and a method (causality and conditions) how to run it. In the next section issue of laser testing is mentioned. Data analysis is described in the last section of this chapter including the ROOT macro which was used.

3.1 Laser Test Setup

In our laboratory we tested DEPFET module H 3.0.11 [1] connected with S3B No. 3 (test system) for readout powered by power supply board No. 19. The measured

[1]This module consists of PXD5 matrix (active area - array of DEPFET pixels), it uses faster Switcher3 chips and CURO2 chips for read out

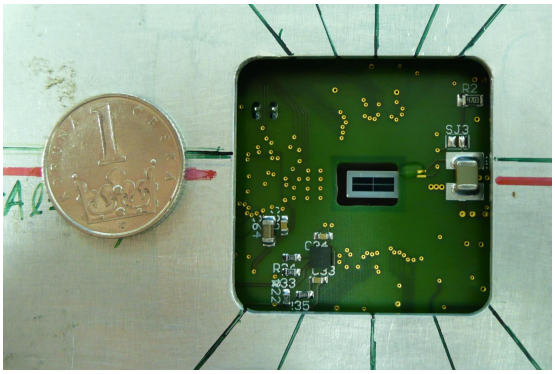

Figure 3.1: The DEPFET sensitive area

sensor had pixels 32 μm times 24 μm in 256 rows and 64 columns. Due to the sensitivity to visible light it was necessary to close the detector in a black box. The sensitive area of the DEPFET module is shown in Figure 3.1 in comparison to one Czech coin. During the measurement the module was fixed in a horizontal position by a threaded rod based construction. There was a need for planparallel position to the plane in which was moving the stage with laser. In Figure 3.2 is a view into the black box, the laser is fixed to the stage moved by engines with step 1.25 μm in both horizontal directions (it is also possible to move the table vertically and to rotate it). The laser beam was produced by semiconductor laser with wavelength $\lambda = 682$ nm, and its energy was set approximately to the energy of MIP[2]. Laser light was transferred through the optical fibre and optical attenuator and then focused by a lense into the spot with σ about 3 μm, but generally the spot doesn't have to be gaussian. The distance between the focusing lens and the sensor plane was approximately 12 mm and stayed constant during the measurement.

The whole scheme of connection is shown in Figure 3.3. The IPNP 03 computer commands the moving engines of the table through USB. Through GPIB it sends commands to a pulse genarator Hewlett Pacard 81101A, which generates 10 ns long pulses for a red semiconductor laser and sends a trigger signal (from trigger out connector) to another pulse generator(Agilent 81110A). The 10 ns long generator pulse generates only about a 3 ns long laser pulse because the laser power

[2]Minimum Ionising Particle - is a particle whose mean energy loss by passing through a matter is close to the minimum. The mean energy loss is primarily a function of velocity β and reaches the minimum value for $\beta\gamma$ between 3 and 4 [13]

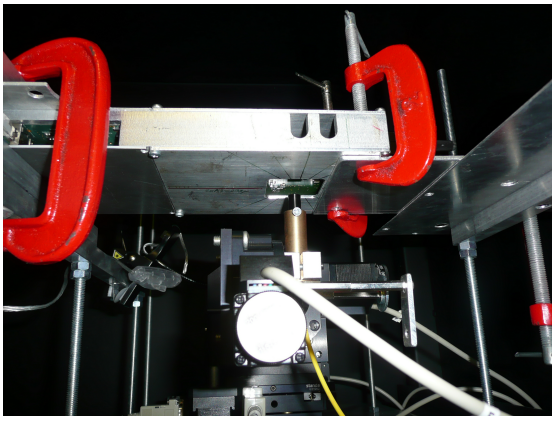

Figure 3.2: Laser test setup in blackbox

increases slowly with excitation (spontaneous emission is dominating) until it approaches the lasing threshold (above this threshold is the power dominated by stimulated emission) and this takes some time, which is in this case of the same order as the pulse length. We had to use the second pulse generator for triggering the DEPFET module because none of available NIM modules were able to give an appropriate trigger signal, which should have the basic level of +50 mV and then a -1.8 V pulse. Outputs from both generators were observed on an oscilloscope. The optical attenuator was also connected to the IPNP 03 computer via COM port. The trigger signal from second generator was managed by TLU, only one out of its eight channels were used, so it would be possible to make a more complicated experiment. From TLU, the trigger signal went by RJ-45 to our module which was then read out by IPNP 72 computer, connected through an S3B test system, through TLU and by USB.

3.2 Software

First of all a sufficient memory space is required in the IPNP 72 computer for the S3B board buffer, at least 200 MB. It is possible to do that only as an administrator in the configuration file:
`/etc/sysctl.d/shmmax.conf`.
It is also necesary to look if a measurement in VNC is already running. At first the IPNP 72 terminal must be opened (for example by PuTTy) and then use the

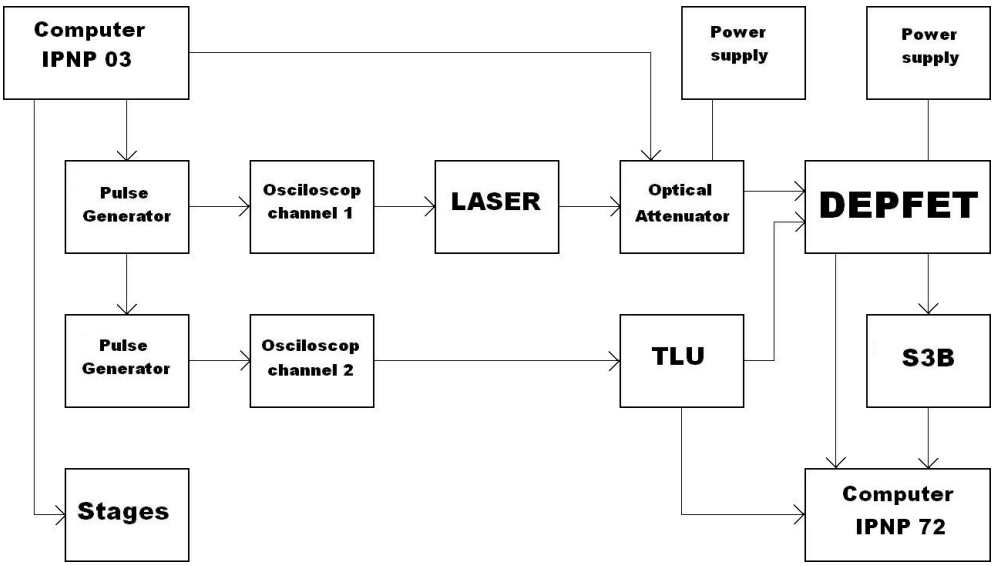

Figure 3.3: The connection of hardware

command:

`ps -ef grep vnc`.

This command finds out if VNC is running. To look at the running measurement, then run:

`vncviewer ipnp72:1.troja.mff.cuni.cz`, otherwise run VNCserver:

`./vncserver`.

The VNC is usefull for remote control the measurement. When VNC is running, it is possible to start programs needed for the measurement itself:

To run the power supply software, through which we can set many different voltages at the detector (see Table 3.2), do following steps:

`cd /PowerSupply/work_supply`,

this browses the appropriate directory, then simply run:

`./runS3BSupply`.

After starting, it is necessary to set up a proper connection, in its menu set: `connect to host "localhost" port 32767`. Then it is necessary to load a configuration file by:

File-Load `./S3BSupply/ini-files/S3b_config_opt_H3011.ini`.

Power supplies can be managed through menubar "File":

- Apply Settings
- Power On / Off

Next DAQSoft is run, which takes care of readouts. If you browse the program directory:

`cd DAQSoft/work_depfet/`

then run the script by command with parameters:

`./START_UP.sh -r -m 1 -d local`,

-r means cold restart, -m 1 means start for one module.

Now fill the fields Server: `localhost`, Port: `32767` and push the (Re)connect buton. Then push the STATUS button and then the INIT button.

For running TLUSoft it is necessary to control the access laws, in the directory:

`depfet@ipnp72: /TLUSoft/tlu_tcp$` run: `./chmod_depfet.sh`

Then run: ./TLUControl.exe -a 1 -d 1.

Such a set of parameters means the usage of external triggers. The last program on the IPNP 72 computer is DQM (Data Quality Monitor), which enables the realtime monitoring of detector response:

`cd DAQSoft/work_depfet/`

`./Monitor.exe -rem=localhost`.

3.2.1 ROOT macros for running the measurements

When everything was runing on the IPNP 72 computer, the last thing needed, is to command the measurement, to manage the pulse generator, optical attenuator and moving stages. For this purpose a few macros were written:

- `Timewindow.cpp`
- `DepfetMatrixXY1.cpp`
- `DepfetmatrixXY2.cpp`.

All these macros, each for a different measurement, use the functions for managing the moving stages from `RunXYZStanda.cpp`, `LTPK_GPIB.cpp`, which manages the pulse generator, and `OpticalAttenuator.cpp`, which rules optical attenuator. Some functions were added to `LTPK_GPIB.cpp` their description is as follows (for more information about the used pulse generators see the manual [14] and reference guide [15]):

- `void SetDEPFETPer(int LTLaserColor = 2, int PulsWi = 10, int HighVSet = 0, float Delay, int Period, int Burst)`

  Its purpose is visible from the name and parameters, by the row: it sets laser color, length of pulse (in ns), amplitude of pulse (in mV), delay of pulse(in ns), period of pulses (in ms) and the number of pulses sent in a row, provided by the pulse generator. From this function the next one is derived.

- `void SetTrig(int Burst, int Delay)`

  This function sets only the number of pulses and pulse delay provided by the pulse generator.

  The new macros are basically similar to the measurement mentioned in section 3.3. In each case, a series of pulses is repeatedly sent by the `DEPFETTrig()` function from `LTPK_GPIB.cpp`, then as a gap they send only the trigger(actually a pulse is sent, but delayed enough) Also in the beginning and at the end of measurement several hundreds or thousands of triggers are sent (for pedestal correction, see section 3.4). For this purpose the pulse isn't delayed in the `DepfetMatrixXY1.cpp` and `DepfetmatrixXY2.cpp` macros, instead the attenuation of laser light is used. These two macros are moving the stages between points and the difference between them is that first one scans the matrix in a row-like fashion and the second one in a column-like fashion. `Timewindow.cpp` makes a series of pulses with different pulse delays.

3.3 Measurement

We planned to do two measurements, first to measure clearing resp. reading frequency by shifting the trigger signal backward resp. forward in time. In every such a point (one different delay of trigger signal with respect to laser pulse) it is necessary to measure enough events to have good statistics for this purpose (a thousand). Another important thing is that the measured interval of trigger shifts is long enough (no hits should be detected in its beginning and at its end). The next is to measure the "edge effect". It means to scan some grid which

contains the edge of DEPFET matrix (about 200 μm wide area by the border). This measurement should be done by each of the edges of the detector (left, right, bottom and top). When everything was connected properly, we started taking data. Although the detector worked 100% in short time measurements, in the case of long time measurements (roughly, 1000 events and more) a problem appeared. When measurement was finished, all the events weren't in the in the data file. We tried it several times and the efficiency of data taking was only $(93 \pm 1\%)$. The system is not made for laser tests, when the S3B board has a full buffer and starts to sending data into the computer, it is impossible to read out the detector matrix. In a beam or source test this doesn't matter, but in the case of well defined laser test it is a disadvantage. What was needed was to distinguish between the detector response in different positions (no matters if spatial or time), because it is impossible to just derive it from the event number. The possibilities were:

- To split the measurement, so one measurement should contain only one point. This hasn't been tried, because it would be time consuming.

- To use a "gap" (several events without hitting the detector matrix) between points, closing the optical attenuator to stop laser light. Actually this was tried, but there can be different responses from detector, because when the optical attenuator is closed and opened again hundreds of times, the accuracy of how much it is opened or closed decreases. Also, it was really time consuming.

- To use a "gap" between points, by delaying the signal enough to be read out the internal gate cleared from before. It is much faster and more pricise than using the optical attenuator.

For every measurement it was necessary to start all the programs on the IPNP 72 computer mentioned in section 2.2 Software and then:

- In the DAQ program push the CONFIG buton, then INIT.

- In the power supplies program switch on the power supplies, apply settings. If some sign is red, switch it off and repeat this.

- In the DAQ program push the start button.
- On the IPNP 03 computer start the ROOT macro (`Timewindow.cpp`, `DepfetMatrix1.cpp` or `DepfetMatrix2.cpp`) which commands the pulse generator, moving stages and optical attenuator.
- When the measurement is finished push the STOP button in the DAQ program.

During all the measurements it is good to watch all of the voltages and the online data in the DQM. In measurements of time properties, the fixed delay was set on the second pulse generator, because it wasn't possible to send a pulse before the trigger. Three measurements were done with the settings written in Table 3.1.

The voltages were set as shown in Table 3.2, 3 ns long laser pulses were generated with frequency 10 Hz. The edge effect was observed in dependence on Bulk Voltage from 4 V to 11 V with respect to the source with step 1 V. By every edge of the detector was a scaned grid of 10 times 30 points (10 points were in the direction parallel with edge). Points were equidistant and the distance between them was 10 μm in both directions. One hundred laser pulses were generated in every point, and ten laser pulses were generated in the gap between them (the laser pulse was a half period delayed).

3.4 Data Analysis

From the read-out software we obtained the row data which contained the data sorted by event number. For each of the events there was a charge collected in every pixel of the DEPFET matrix in ADU (Analog to Digital Unit). On such a data set the pedestal correction and common mode correction were done, the

No.	min. del. [μs]	max. del. [μs]	step [μs]	ev. in point	ev. in gap
1	-100	100	2	1000	100
2	-5	5	0.1	1000	100
3	0	3000	10	1000	100

Table 3.1: Time properties measurement

Contact	Voltage [V]	Contact	Voltage [V]
Source	7.0	Bias	180
Bulk	16.0	CCG	6.6
Gate On	1.6	CURO A	2.5
Gate Off	9.6	CURO D	2.5
Clear On	20.5	TIA+	2.8
Clear Off	10.0	TIA-	0.8

Table 3.2: DEPFET Voltages

pixel charge noise is 15 ADU, which is standard deviation σ of charge distribution (counted from events without hits). The next step was to find seeds, each given by a pixel with the highest charge in its neighbourhood, to which a cut was applied, we took only those with SC (Seed Charge) higher than 100 ADU. Then it was necessary to find a whole cluster, pixels in 7 times 7 square with seed in the middle, whose charge was at least 39 ADU (2.6σ threshold). For such a Cluster the COG (Center Of Gravity) position was counted (center of gravity of pixel in the cluster weighted by their charge). Also CC (Cluster Charge) - it is the sum of all charges above a 2.6σ threshold in the 7 times 7 square - and CS (Cluster Size) - the number of pixels with collected charge above a 2.6σ threshold in the same square - were counted. All the processed data were written into a .asc file for every run. In such a file, for every hit in every event (usually was one hit per event) the following were recorded, its position (x and y), seed charge, cluster charge, cluster size and the doublerow number where the reading started.

The next step was to recognize events which belong to some point (set of events with constant laser position and pulse delay) and which belong to the next one. For this purpose the gaps (10 events with pulse delayed with respect to trigger, then nothing was detected, see Figure 3.4) were put in the measurements. Especially in time measurements, it was really important to recognize even where the point ends and the gap starts, because the goal was to obtain the probability of detection with a specific delay of the laser pulse. So we need to know how many hits and "how many triggers were detected". One artefact of readout was helpful,

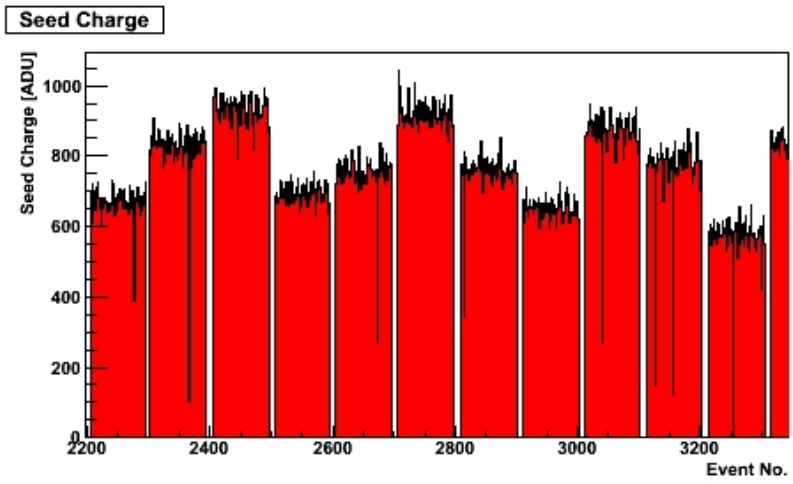

Figure 3.4: Seed charge as a function of event No., the "gaps" between "points" are visible here.

although it stayed unexplained. In first event of the series (no matter if point or gap), there was an additional hit in the column No. 62 of doublerow, where the readout started. Or in the beginning of the line of points (row or column in edge scans) there were about ten additional hits in the doublerow, where the readout started. These artefacts were observed in every run (comparison between the hitmap with and without these hits is in Figure 12). For the arrangement of experimental data to an easily readable form MS Excel was choosen, in which were the gaps clearly identified by missing event numbers, proper number of events in between and artefacts mentioned above.

When the data were arranged in MS Excel to easily readable form, they were read by the macro `LTAnal.cpp`. This macro split the data by points as the stages were moving. Then a cut of CS was applied, because sometimes the laser hit some optical dust on the plane, which reflected the laser light all around (even events with CS higher than 40 were observed). From this data several histograms were created. For every run (measurement with specific value of bulk voltage by one of borders) the histogram of CC, SC, CS and $\frac{SC}{CC}$ was created, an example is shown in Figure 3.5 (all of them are stored in electronic package of this thesis). The CC and CS distributions are the same as in Figure 3.5, only the histograms (merged from all the edges) of seed charge by different bulk voltages are shown in Attachement as a Figure 11. For every point the medians of reconstructed position (both directions independently), seed charge, cluster charge and the arithmetic mean

of cluster size were counted. Statistically, the median has a relatively high error $\approx \sqrt{n}$, but for this purpose it is a better choice than the mean due to distant "tails". In case of CS, the mean is reasonable, as the distant "tails" were cut out. In the next step, the position of the stages was subtracted from the reconstructed position (approximately, the area of the closest points to the middle of matrix was taken as reference, so the misposition in these points is around zero). This subtraction is done to the constant, the most important is the relative misposition of two points (absolute value can be chosen[3]). From this data the 2D plots of misposition in direction perpendicular to appropriate edge and cluster charge as functions of laser spot position were made and they are shown in Attachment in Figures 1-6. An example (Misposition plots, cluster charge, seed charge, cluster size and number of hits in a single "point" by left edge with 6 V bulk voltage) is in Figure 3.6. For better statistics which isn't influenced to much by in pixel distribution the mean of all the "point" values (misposition, CC, SC, CS and number of hits) by the same border obtained from the measurement with the same bulk voltage in the same column / row (parallel with the apropriate edge) was counted. For better comparison of misposition graphs by the same edge but with different bulk voltages, there was for each subset one value (for all subsets this value has the same laser spot position in the direction perpendicular to the edge) taken as reference. The laser spot position where the misposition values (of different subsets) were closest to each other was chosen. Misposition in perpendicular direction, cluster charge, seed charge and cluster size for different bulk voltages are then shown as a function of laser spot position in the perpendicular direction to the appropriate edge in Figure 4.1-4 (there are only four subsets in one graph, the step in bulk voltage is 2V, graphs with all the subsets are shown in Attachments in Figures 7-10).

For the whole analysis of time properties measurement, MS Excel was used. As the cluster charge for all reconstructed hits was fluctuating by noise and the laser

[3]Although used constants are reasonable, because the misposition in average over some area (big enough, that it is not affected by inner pixel distribution of hits) far from the edge should be approximately zero

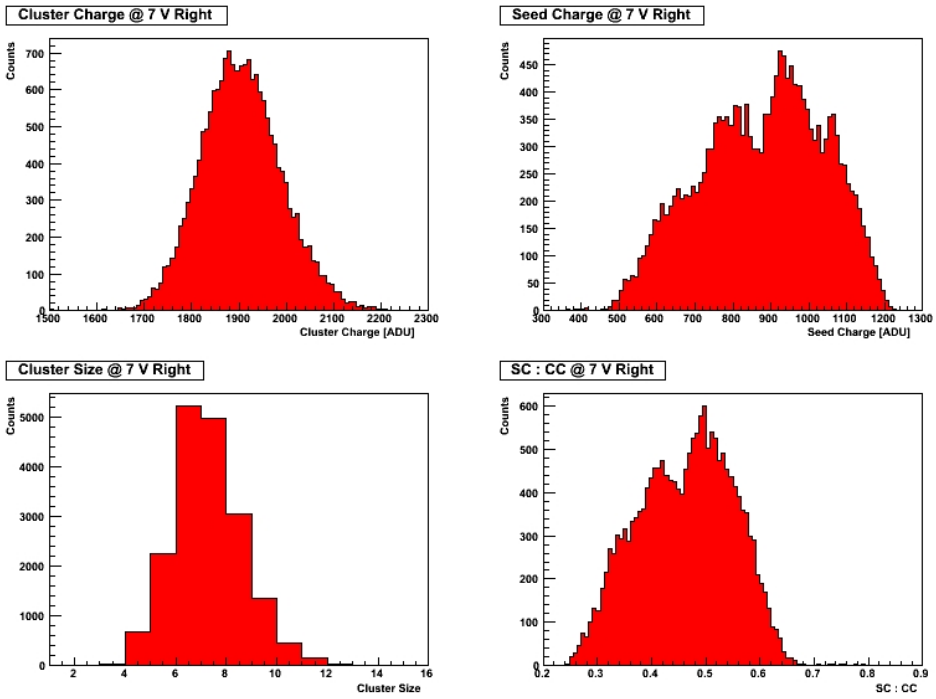

Figure 3.5: Histograms show the distributions of CC, SC, CS and SC/CC by right border with a bulk voltage equal to 5 V with respect to source.

position stayed the same, hits were used only like binary information.[4] Using the gaps and artefacts mentioned above the number of detected hits and number of detected triggers were derived from the data. Then the probability of detection as a ratio between the number of detected hits and the number of detected triggers for every specific pulse delay was counted. The error was counted as the error of a Poisson distribution, because it is a stochastic process. This way the probability of detection as a function of pulse delay was obtained, which is shown in Figure 4.5. Then the upper limit of no detection probability and lower limit of sure detection were counted by linear regression of the rising part. The interval between them is a period of time needed for clearing the whole matrix. In the same way the upper limit of sure detection and the lower limit of no detection probability were obtained, the only difference was that linear regression of the decreasing part of dependence was used.

[4]There were only a few hits with significantly smaller cluster charge, what could correspond to readout during the period of charge collection. With this statistics it couldn't be taken into account.

3.4.1 ROOT macros for analysis

This part of analysis was implemented into ROOT, the macro `LTAnal.cpp` was prepared. It uses functions from its header file `LTAnal.h` and the important ones of these are as follows (for explanation of terms and better explanation what and why it was done, see sections 3.3-4.), for details about ROOT, see [16]:

- `void Configure(int RunNo)`

  Sets the working variables for specific run, run number is a parameter of this function.

- `void Init(void)`

  Sets the variables used by other functions, run just once.

- `void LoadData(int RunNo)`

  Loads the pre-processed data (COG positions, cluster charge, seed charge, cluster size, event number and hit number) from .asc file for just one run specified by run number. Also, a cut on cluster size is done, mentioned above.

- `void ProcessData(void)`

  In this function medians of COG position, cluster charge and seed charge are counted from the data in every "point" of the actual run. The means of cluster size values are counted in every "point" too.

- `void ProcessData2(void)`

  For all the loaded and processed data (there is only one value of a kind per "point") from runs done by actually set border, it counts the average values for "points" in the same column/row (the laser spot position) parallel with the appropriate edge. Also laser spot positions (coordinates of moving

stages system, to the constant) are subtracted from reconstructed positions.

- `void Plots(void)`

  This function makes 2D plots of x and y mispositions, cluster charge, seed charge, cluster size and number of hits in one point in dependant on laser spot position. These plots are done for all runs by the actually set edge. The plots are saved into .gif files.

- `void Hists(void)`

  This function creates, fills and saves into a file the cluster charge, seed charge, cluster size and $\frac{SC}{CC}$ histograms for all hits in every one run (the same border and the same bulk voltage), from them merged histograms are created for each value of bulk voltage. A hit map for all runs together is also created.

- `void ProcessData3(void)`

  This function subtracts an averaged displacement of some point as close to the middle of matrix as possible, where the values for different bulk voltages are closer, from all the averaged positions in different distances from the edge.

- `void SummaryPlots(int th)`

  The final multi-graphs of displacement in the orthogonal direction to the appropriate edge are created, then of seed charge, cluster charge and cluster size. There is a line drawn for every specific bulk voltage. The parameter equals the step of bulk voltage (if it is higher, less lines are drawn... this is good for visibility).

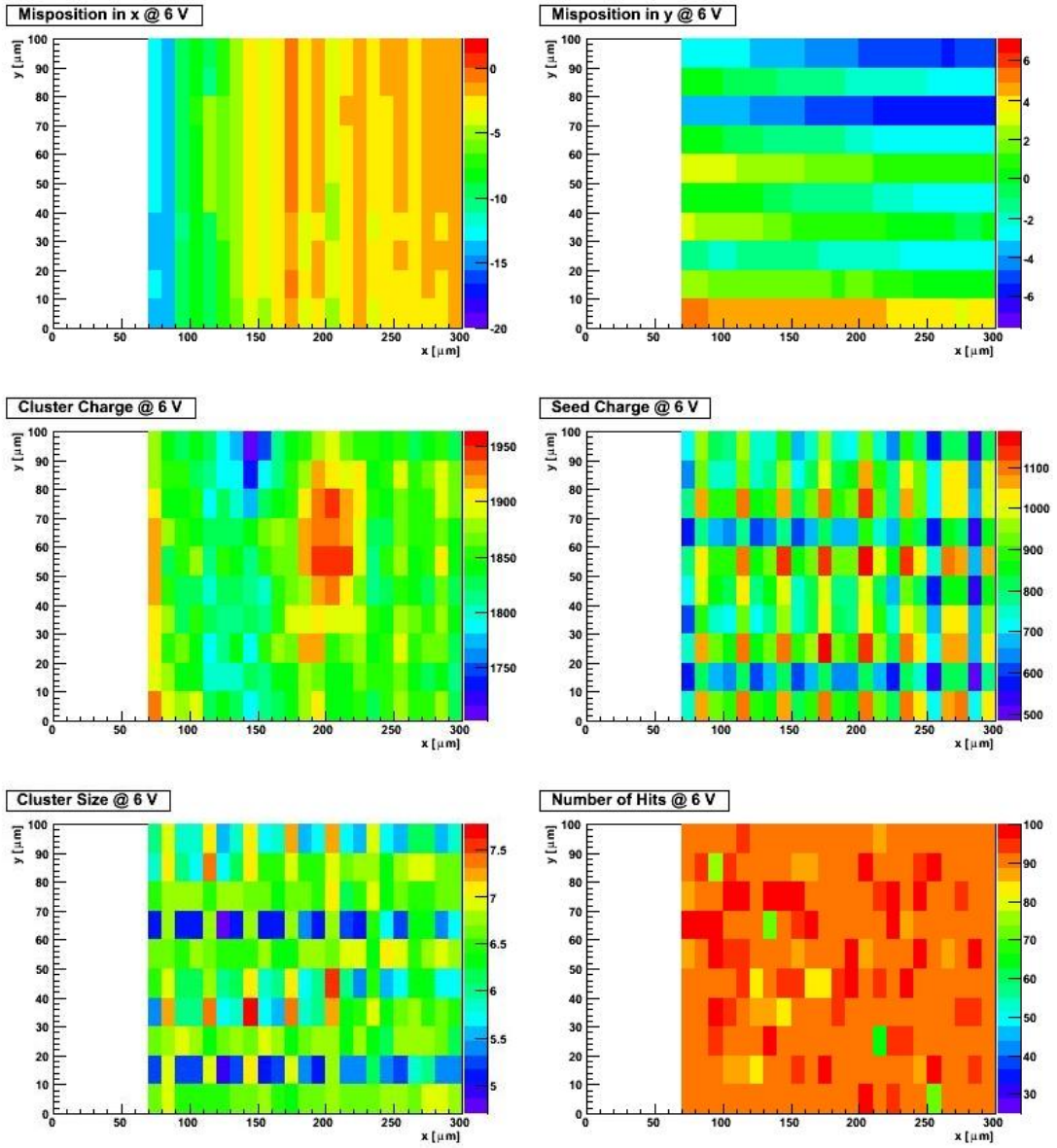

Figure 3.6: All plots show the data from left border with bulk voltage 6 V with respect to source as a function of laser spot position. The displacement plots (top) show the difference between the calculated COG position and the laser spot position, the colour scale unit is 1µm. The charge distributions are in the middle and in the bottom the cluster size and number of hits are shown.

4. Results

The results of the laser test are presented in this chapter. The comparison with test beam results can unfortunately be done only for the central part of the detector, however it is mainly a comparison of testing methods. Section 4.1 describes the edge effect results. In section 4.2 the speed of the detector readout is mentioned and in the last section the laser test results are compared to the beam test results.

4.1 Edge Effect

In this section the results of edge scans with bulk voltage in the range from 4 V to 11 V (with respect to source) are presented. The scan results of the left, right, top and bottom edges are shown in a row in Figures 4.1-4. Subsets shown in these figures correspond to different bulk voltages with step 2 V (for clarity, figures with all the subsets you can see in attachment as Figures 9-12). In Figures 4.1-4 a subset of data is shown for (bulk voltages are with respect to source):

- 4 V - light blue, full circles
- 6 V - dark blue, full triangles
- 8 V - light red, empty circles
- 10 V - dark red, empty triangles

Up to now a bulk voltage from 9 V to 10 V with respect to source was used (dark red line with empty triangles). The edge effect is visible approximately up to the eighth or maybe up to the tenth pixel from the edge. The misposition (difference between the counted COG position and the laser spot position) increases with decreasing distance to the border, by lower bulk voltage a big improvment is visible and even the additianal point closer to the border was detected (it means 10 μm closer). When the corresponding points closest to the border are compared (the same distance of the laser spot position from the edge), then in the worst

case the edge effect is twice smaller (by left border four times, by right border two times, by top border two times and by bottom three times lower, all with respect to 10 V). By the top and bottom edge "shifts" are visible of typical shape of in-pixel misposition [1] by edge effect. Cluster charge distribution is differenf by the in-pixel position, when the hit is in the middle, CC is the smallest, at the edge of pixel CC is higher and in the corner CC is the highest due to charge division among pixels and due to charge threshold (the variation is few times bigger than threshold). Local inhomogenities of Si-bulk and refraction or reflection can influence the cluster charge distribution, in such a case there isn't visible any regular structure. By top and bottom edge of matrix is visible the leak of charge close to the edge, this is also fixed by decreasing bulk voltage. This effect is not visible by left and right edge, because it is fixed by additional outer ring in these parts of DEPFET matrix. By the right edge with 4 V bulk voltage was observed cluster charge about 3% lower with respect to the average of others. The seed charge distribution is strongly dependendent on in-pixel position, in the middle SC is the highest, by middle of pixel edge it can decrease to half and in the corner it can decreases to quarter (these are theoretical limits) due to charge division among pixels. In graphs are smaller differencies (the height of serration), because it is averaged in one direction and the cluster size is bigger than for theoretical limits. The cluster size distribution is influenced by charge division too, for constant size of produced charge cloud in the detector bulk is the line in graph seratted too. As in misposition graphs is a "shift" of shape, there is seen the change of shape in seed charge and cluster size distribution by bottom and top border (it is because of small non-integer ratio between the step and pixel size in y-direction, so the serration is iregular).

4.2 Time Properties

The probability of detection as a function of laser pulse delay is shown in Figures 4.5-6. The graphs are shown without error bars, in Figure 4.5. The errors are smaller than markers and in Figure 4.6 we have ommited them. it is for clarity

[1] Due to the charge division between pixels and threshold for pixels in cluster, with the step of 10 μm the lines are (in misposition graph) only serrated

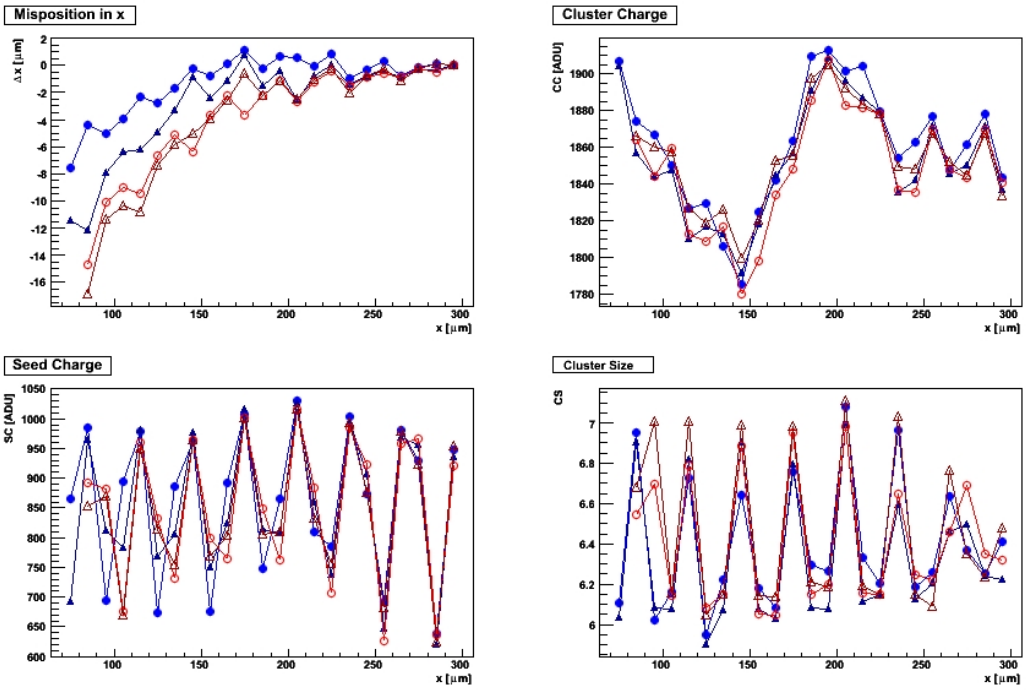

Figure 4.1: The graphs from left show the mean of corresponding values with the same distance (of laser spot) from the border as a function of laser spot position. The edge is on the left side of graphs. For description see the text of this section.

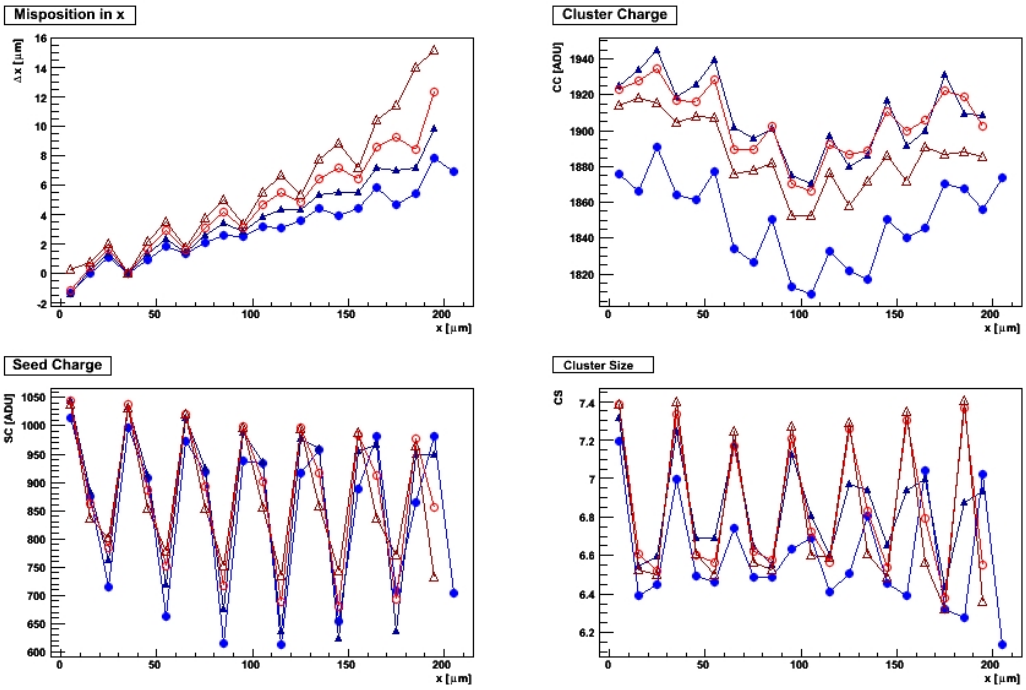

Figure 4.2: The graphs from right show the mean of corresponding values with the same distance (of laser spot) from border as a function of laser spot position. The edge is on the right side of graphs. For description see the text of this section.

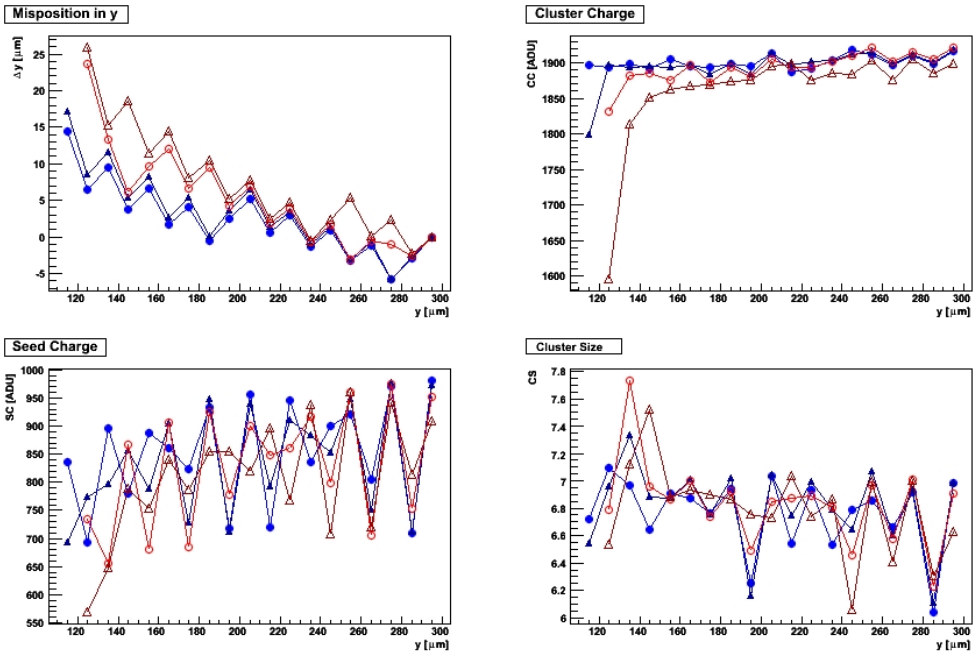

Figure 4.3: The graphs from top border show the mean of corresponding values with the same distance (of laser spot) from border as a function of laser spot position. The edge is on the left side of graphs. Description of seen effects is in text of this section.

reasons. The left part of Figure 4.5. shows clearing of the DEPFET matrix. The time points, correspond to hits not being cleared before reading. The trigger fires at pulse delay 0 μs. We can see that the probability dependence between the latest point where the probability of hit detection is 0 and the point where trigger fires has a linear dependence. The right part is focused on readout, there is the probability dependence linear up to the time point when whole matrix was read out before the trigger fire. From this data the clearing and readout times are derived, see Table 4.1.

	Clearing time [μs]	Readout time [μs]
Whole matrix	(54 ± 1)	(2320 ± 10)
One doublerow	(0.42 ± 0.01)	(18.1 ± 0.1)

Table 4.1: Clearing and readout time

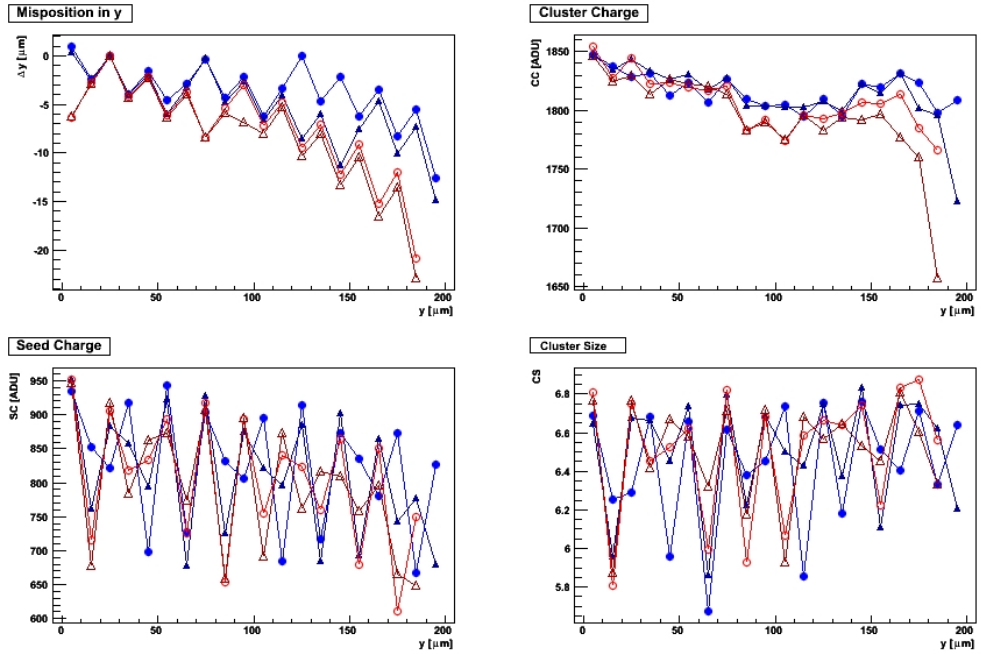

Figure 4.4: The graphs from bottom border show the mean of corresponding values with the same distance (of laser spot) from border as a function of laser spot position. The edge is on the right side of graphs. Description of seen effects is in text of this section.

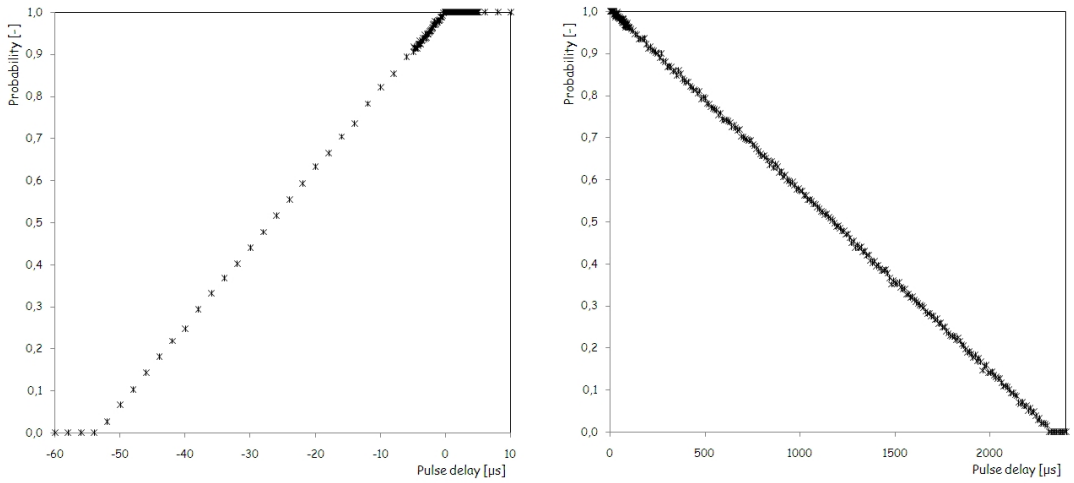

Figure 4.5: The probability of hit detection in dependence on laser pulse delay: Left graph coresponds to the rising part (by increasing pulse delay, the smaller part of matrix is cleared in the meantime) and right graph coresponds to decreasing part (by increasing pulse delay, the larger part of matrix is readout, before the pulse fires).

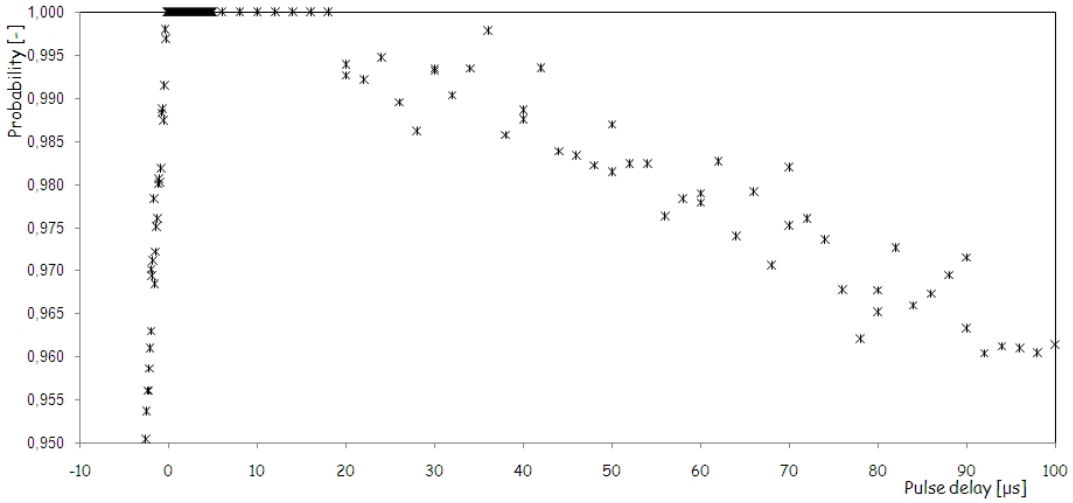

Figure 4.6: The probability of hit detection in dependence on laser pulse delay - sure detection plateau

4.3 Comparison to Beam Test

In this section the cluster charge and seed charge "maps" of the same area of the same module are compared. In laser test there was occupancy approximately 5000 seeds per pixel against 260 seeds per pixel in results from beam test at CERN in 2009. The plots from laser test data are shown in Figure 4.7 and from test beam data in Figure 4.8. The areas with larger collected charge are marked by red circle. The area where the collected charge gets lower is signed by blue line. The good agreement is clearly visible in cluster charge plots. The same areas marked in seed charge distribution from beam test and they correspond to lower resp. higher seed charge. The main visible effect from laser test is in seed charge plot is the dependence on in-pixel position.

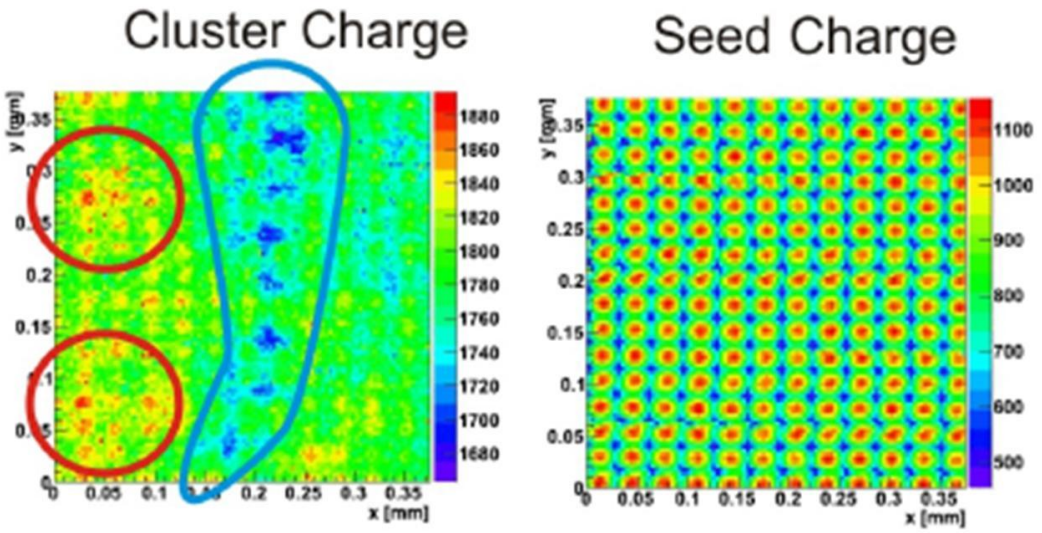

Figure 4.7: Cluster charge and seed charge distribution in central part of DEPFET matrix created from laser test results, occupancy is approximately 5000 seeds per pixel and peak to peak variation is about 4%. Courtesy of Peter Kodyš

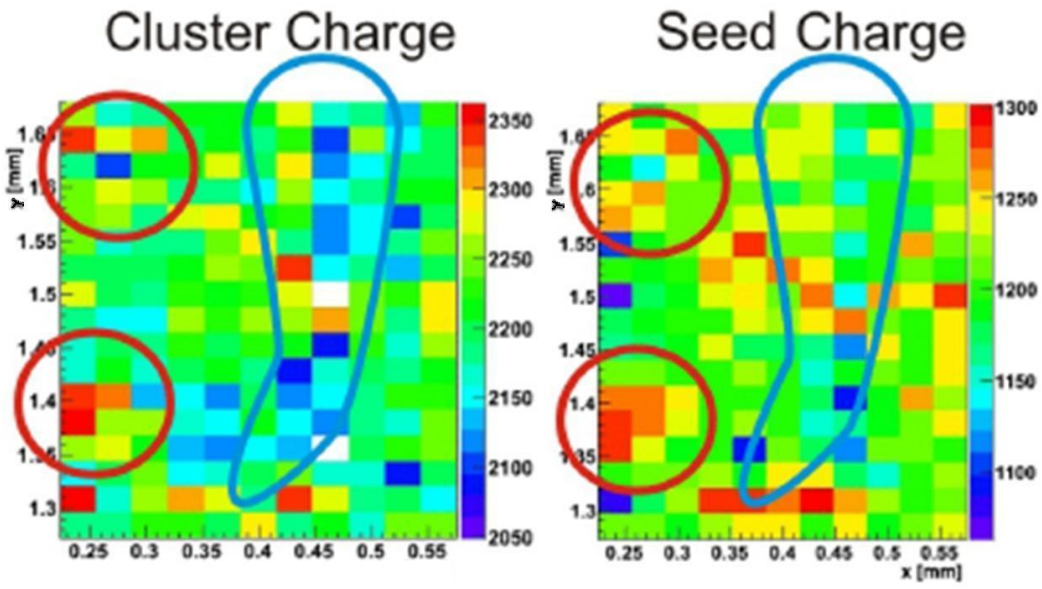

Figure 4.8: Cluster charge and seed charge distribution in central part of DEPFET matrix created from beam test results from CERN 2009, occupancy is approximately 260 seeds per pixel and peak to peak variation is about 15%. Courtesy of Peter Kodyš

5. Discussion

We are now going to discuss results, their errors and where they can come from. In case of edge effect the errors haven't been mentioned yet, because it is not in the scope of this thesis. There are several possible sources of errors, as only the border area where the edge effect is visible, there is no possibility to make an η- correction with used step density (2.4 steps per pixel in y-direction and 3.2 steps in x-direction), because it is not seen the laser spot in the same or at least close in-pixel position enough times, to subtract the main in-pixel effects which cause the serration of lines in all the graphs Figures 4.1-4 (some of them are not serrated, but actually this is the defect). Used step density is good enough to fit the mean value of misposition in area not so close to the edge, where the dependence isn't steep. On the other hand, the error in one point (median of set of values in one laser spot position) can be calculated, but when the function (no matters if misposition, cluster charge, seed charge...) is fit, there would be a large number of points which don't fit it in order of calculated error, because not the only one effect is observed. The possible solution, how to subtract the in-pixel effects is to measure more points with finer step, to see both effects more precisely and then split them (it would be like superposition of some monotonic function and periodic function). However, this means to make much more moves of stages, which increases the error in laser spot position, it makes the time of measurement longer, so there rise up a need for stability of physical and mechanical condition in longer time, especially temperature and humidity. It is possible to do that, but in that case, laser test loses its lightweight setup.

Lets summarise the main errors, the error of laser spot position can be estimated from above by 1 μm, so it is still better than several μm from in-pixel effects, this can be estimated from misposition in direction parallel to appropriate edge as 4 μm. The other thing is, that it is needed to take into account the resolution of DEPFET detector, this can be estimated from above by 2 μm. So it would be better and more precise to do the measurement with finer step, but obtained results are convincing even if it is not taken into account that there exist "some" in-pixel effects (it means the error of misposition is about 4μm).

In time properties measurement, no errors come from position measurement, because it is not used. There are statistical errors of Poisson distribution (y-axis of Figures 4.5-6) and errors of pulse delay, they are mentioned in Table 3.1. The point of this measurement is to understand what is happened there. As DEPFET module works it is clearing double-row after double-row and at the moment, when trigger comes, starts readout double-row after double-row. When pulse comes before a trigger, the matrix is still cleared and the probability of detection decreasing linearly in time (it corresponds to double-rows which remain unclear, when trigger comes). So the rising part corresponds to period of clearing the matrix. When trigger comes, there is some time in which is sure detection (at least in case of principle of readout) in this time in the gate on and clear is off, so the charge remains at internal gate (this corresponds to sure detection plateau as it is called in Figure 4.6). That time is readout time of one double-row and together with time length of decreasing part give the readout time of whole matrix (read + clear). As a control we have the ratio between the range of delay where the probability isn't zero and the range of delay where the probability is equal to one. This ratio equals 128 within the experimental error as it should be (the number of double-rows).

Conclusions

Analyzing data from the DEPFET detector we have observed that the size of the edge effect differs with bulk voltage. We have shown that misposition on edges is reduced by decreasing the bulk voltage, for example at 4 V with respect to source the misposition is reduced by a factor of 2 or more, see left top graph in Figures 4.1-4.

At higher bulk voltage we have also observed a leak of cluster charge at top and bottom borders, but with decreasing bulk voltage this leak disappears. A big improvment occurs at 4 V with respect to the source, see right top graph in Figures 4.1-4.

The seed charge and cluster size distributions are at least the same or maybe better with low bulk voltage. As a result using low bulk voltage (4 V with respect to source) is recommended, see Figures 4.1-4 for more details. Readout cycle time properties were measured and the results are shown in Table 4.1, the shape of dependence (Figure 4.5-6) is as it was expected.

The laser test results of the edge effect are in good agreement with the beam test results, they are even more precise due to twenty times higher seed occupancy, see Figures 4.7-8. Laser test is useful for measurement of gain variation between pixels. The results of edge effect measurement were presented on the 5th International Workshop on DEPFET Detectors and Applications and later it was published in [1].

References

[1] Andricek L., et al., *Nucl.Instr.and Meth.* **A** (2011), doi:10.1016/j.nima.2011.02.015

[2] Grupen C., Shwartz B.,*Particle Detectors*, Cambridge Univesity Press, New York, 2008.

[3] LHC machine, *LHC Homepage*, <http://lhc.web.cern.ch/lhc/>, August 2011

[4] KEK, *B - Factory* <http://www.kek.jp/intra-e/research/B-Factory.html>, August 2011

[5] Moser H. G., *Silicon Detector System in High Energy Physics*, Progress in Particle and Nuclear Physics **63** (2009) 186-237

[6] CMS, *CMS experiment*, <http://cms.web.cern.ch/cms/index.html>, August 2011

[7] Kemmer J., Lutz G., *Nucl.Instr.and Meth.* **A 253** (1987), 356-377

[8] Kemmer J., Lutz G., et al., *Nucl.Instr.and Meth.* **A 288** (1990), 92-98

[9] Lutz G., *Semiconductor Radiation Detectors*, Springer, Berlin, 1999.

[10] Doležal Z., Uno S., *Belle II TDR*, Belle group, April 2010

[11] Spieler H., *Semiconductor Detector Systems*, Oxford Univesity Press, New York, 2005.

[12] Andricek L., et al., *DEPFET Pixel Vertex Detector for the ILC*, DEPFET Colaboration, 2007

[13] Bock R.K., Vasilescu A., *The Particle Detector BriefBook*, Springer, Berlin, 1998.

[14] Agilent Technologies, *Reference Guide - Agilent 81110A* <http://cp.literature.agilent.com/litweb/pdf/81110-91021.pdf>, August 2011

[15] Agilent Technologies, *Quick Start Guide - Agilent 81110A* <http://cp.literature.agilent.com/litweb/pdf/81110-91020.pdf>, August 2011

[16] Brun R., et al., *ROOT - A Data Analysis Framework* <http://root.cern.ch/drupal/>, August 2011

List of Tables

3.1 Time properties measurement 18
3.2 DEPFET Voltages 19

4.1 Clearing and readout time 29

List of Abbreviations

ADC	-	Analog to Digital Converter
ADU	-	Analog to Digital Unit
CC	-	Cluster Charge
CMS	-	Compact Muon Solenoid
COG	-	Center Of Gravity
CS	-	Cluster Size
CURO	-	CUrrent Read Out
DAQ	-	Data AcQuisition
DHP	-	Data Handling Processor
DQM	-	Data Quality Monitor
DEPFET	-	DEpleeted P-channel Field Effect Transistor
HEP	-	High Energy Physics
ILC	-	Internationational Linear Colider
LHC	-	Large Hadron Collider
MIP	-	Minimum Ionising Particle
MOS	-	Metal-Oxid-Silicon
MOSFET	-	Metal-Oxid-Silicon Field Effect Transistor
SC	-	Seed Charge
TLU	-	Trigger Logic Unit

Attachments

Attached Figures 1-4 are 2D plots of misposition (difference between counted COG positions and the laser spot position)in direction perpendicular to appropriate edge. With the lower bulk voltage the edge effect decreases, see the edges in the plots there is smaller absolute value of misposition (the sign differs by the opposite edges).Even the additional hits closer to the edge are measured (there are more bins filled in the plot).

Mispositions and CC were produced as median of values corresponding to the same laser position. Cluster Charge leak observed by the top and the bottom edge with higher bulk voltage, disappears with decreasing bulk voltage, see Figures 5-6. In Figures 7-10 are shown the summary plots of displacement (in the direction perpendicular to the edge), SC, CC and CS, containing the means of all the data (this means eight lines, one for one specific bulk voltage) with the same distance of laser spot from the appropriate border. They are better to compare, but on the other hand, the overview becomes worst by a large number of lines. For description see the section 4.1. The SC distribution from the edge scans splited by the bulk voltage is show in Figure 11. The detector inhomogenity and in-pixel effects influence the seed charge distribution much more than decreasing bulk voltage. The artifact used for spliting the points and gap is shown in a one run hit map in Figure 12, for comparison the Figure contains also the hit map from the same run, but without the artifact.

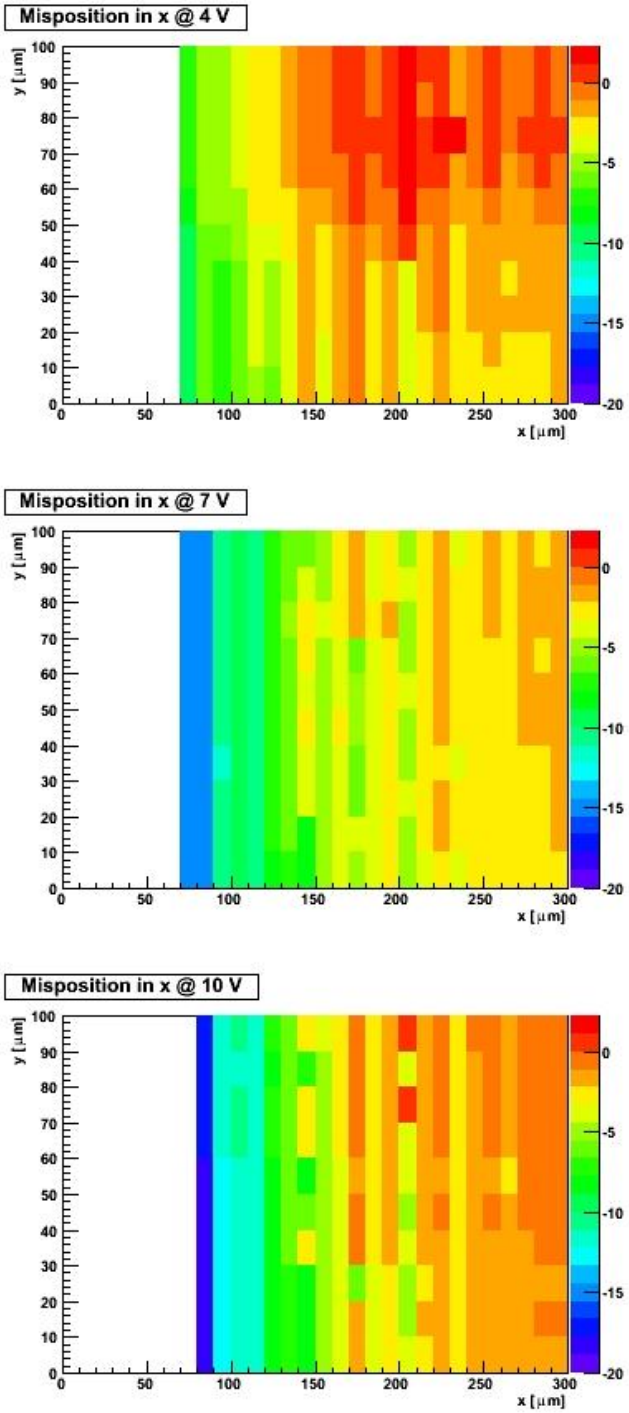

Figure 1: The displacement plots show the difference between the calculated COG position and the laser spot position (in x-direction) by the left edge of DEPFET matrix as a function of laser spot position. The colour scale unit is 1µm. The plots are created from data measured with different bulk voltages, from 4 V to 11 V with respect to source.

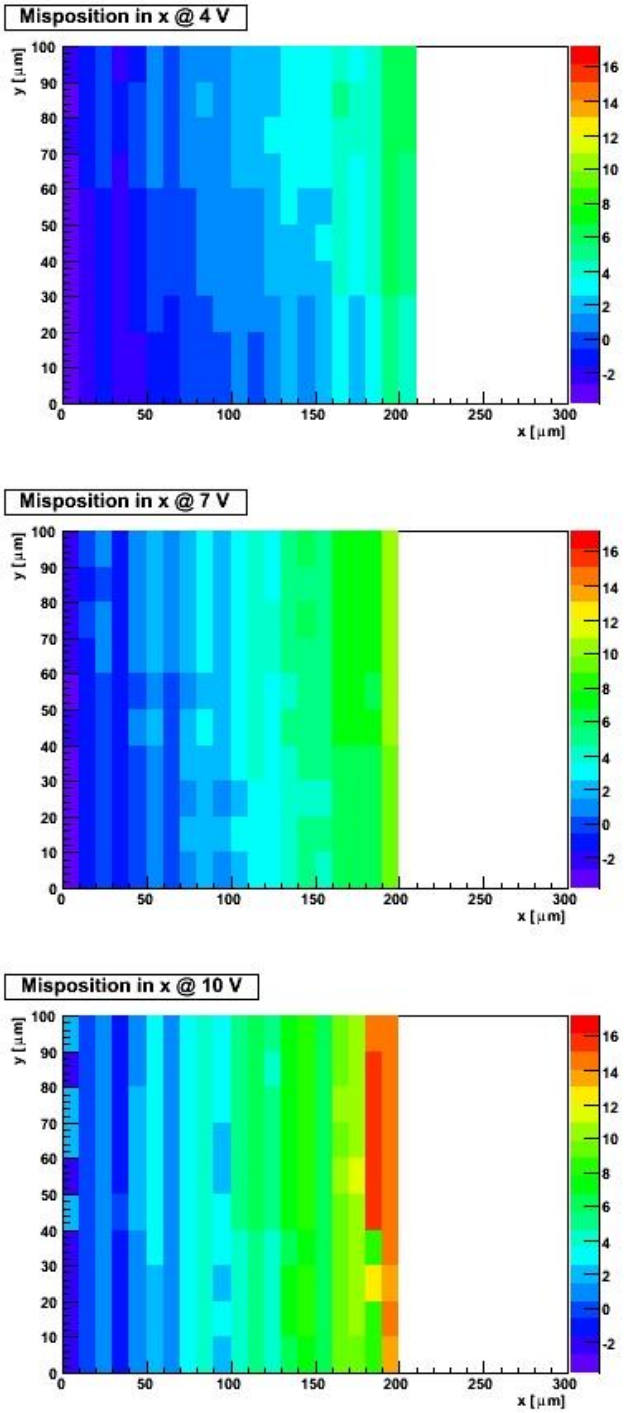

Figure 2: The displacement plots show the difference between the calculated COG position and the laser spot position (in x-direction) by the right edge of DEPFET matrix as a function of laser spot position. The colour scale unit is 1µm. The plots are created from data measured with different bulk voltages, from 4 V to 11 V with respect to source.

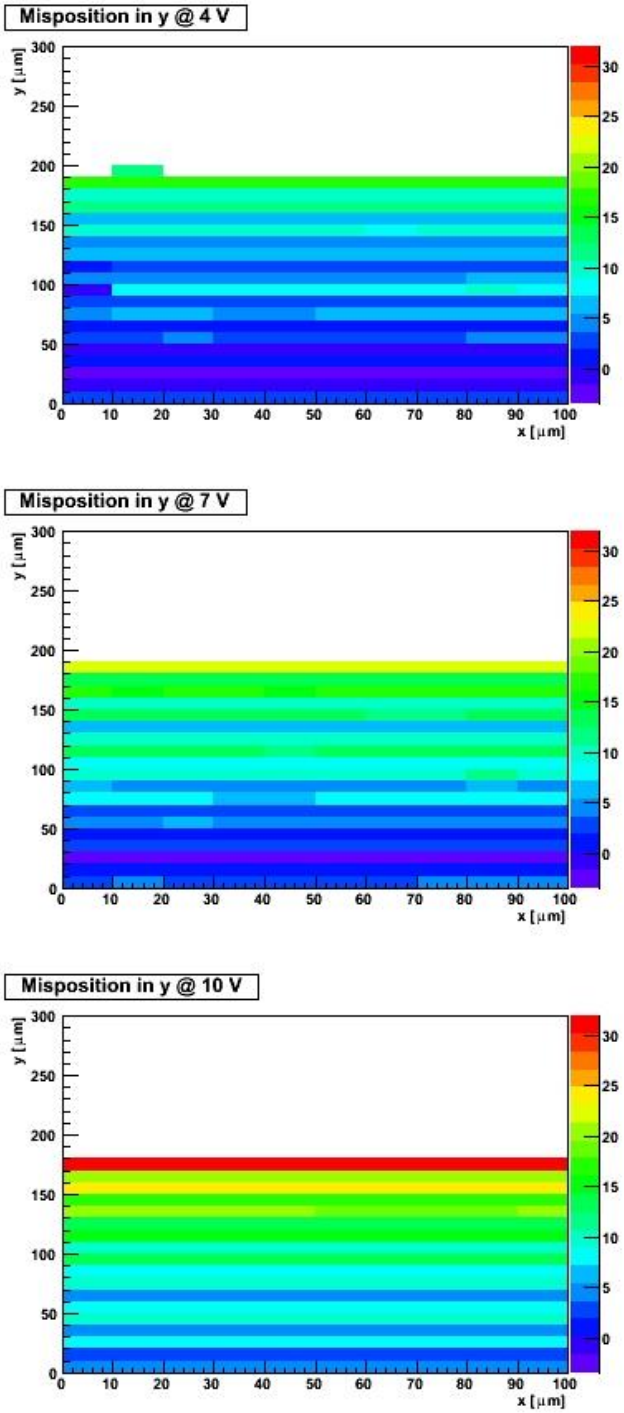

Figure 3: The displacement plots show the difference between the calculated COG position and the laser spot position (in y-direction) by the top edge of DEPFET matrix as a function of laser spot position. The colour scale unit is 1µm. The plots are created from data measured with different bulk voltages, from 4 V to 11 V with respect to source.

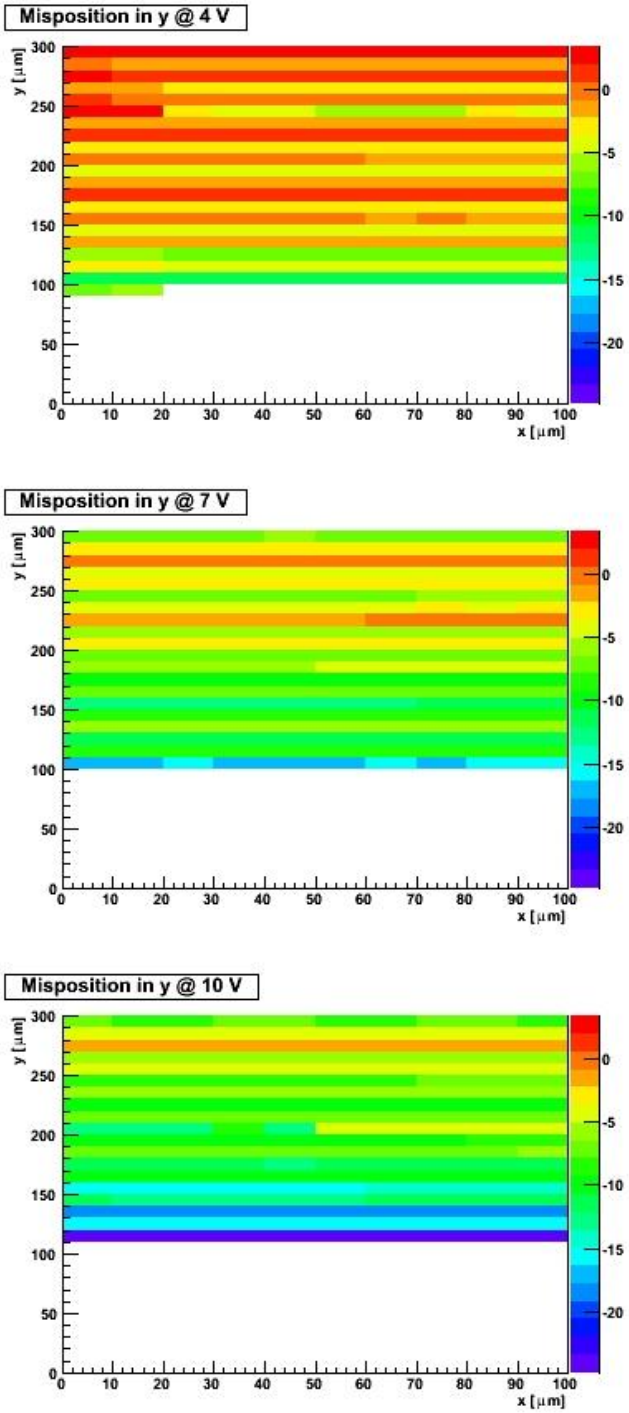

Figure 4: The displacement plots show the difference between the calculated COG position and the laser spot position (in y-direction) by the bottom edge of DEPFET matrix as a function of laser spot position. The colour scale unit is 1μm. The plots are created from data measured with different bulk voltages, from 4 V to 10 V with respect to source.

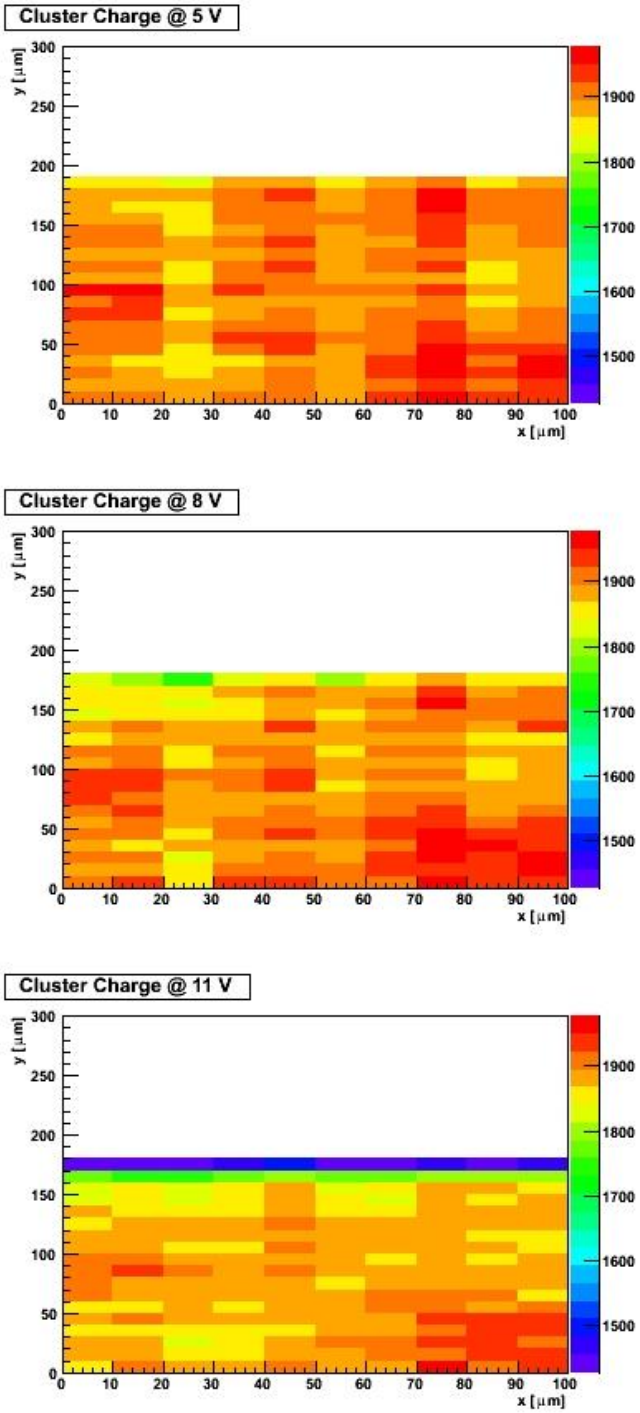

Figure 5: The plots show the cluster charge calculated from the data by the top edge of DEPFET matrix as a function of laser spot position. The colour scale unit is ADU. The plots are created from data measured with different bulk voltages, from 4 V to 11 V with respect to source. We can see the leak of charge with higher bulk voltage. The leak of charge with lower bulk voltage disappears.

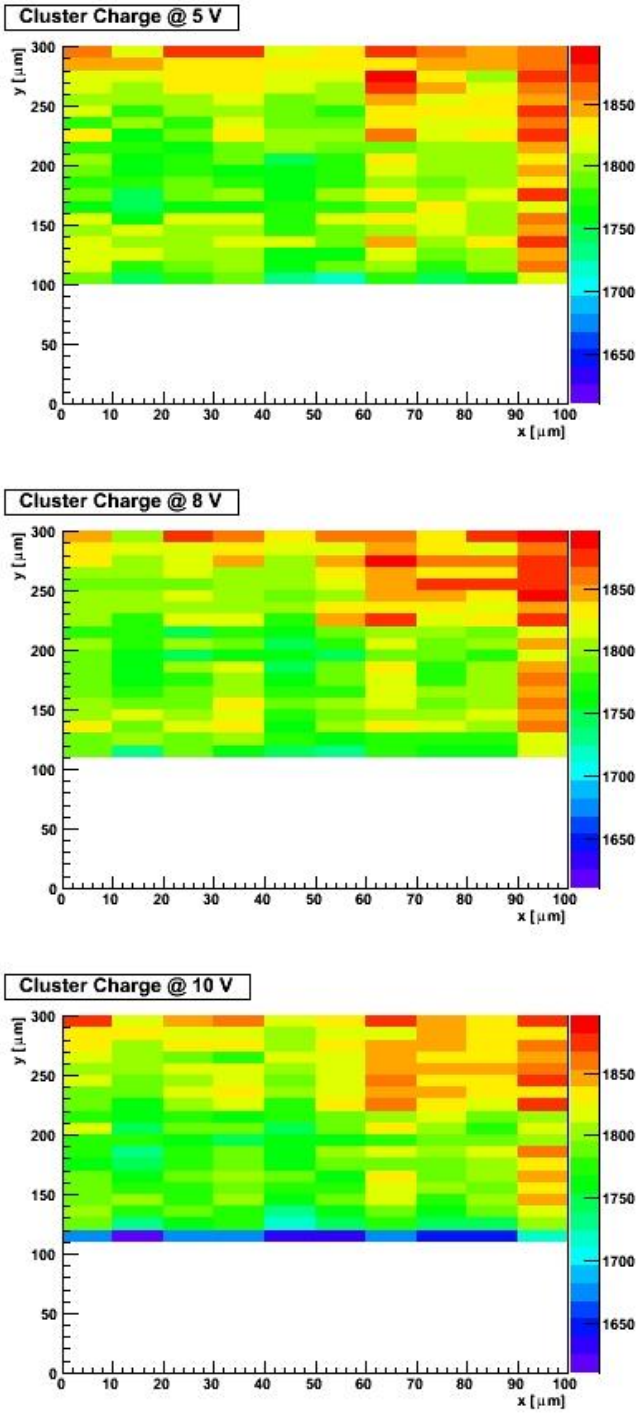

Figure 6: The plots show the cluster charge calculated from the data by the bottom edge of DEPFET matrix as a function of laser spot position. The colour scale unit is ADU. The plots are created from data measured at different bulk voltages, from 4 V to 10 V with respect to source.We can see the leak of charge with higher bulk voltage. The leak of charge with lower bulk voltage disappears.

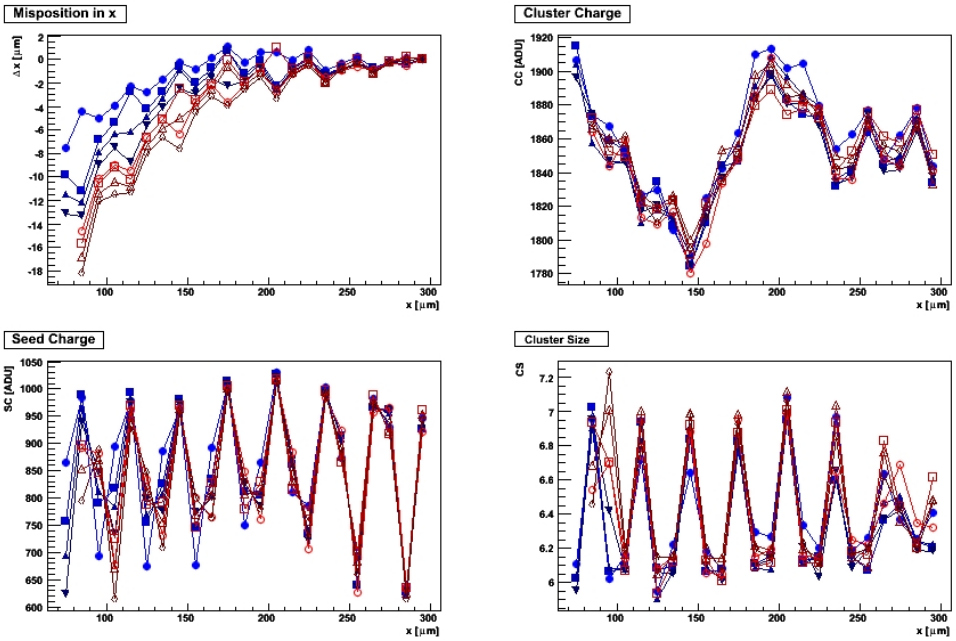

Figure 7: The graphs from left border show the mean of values with the same distance(of laser spot) from border as a function of laser spot position. A subset of data is shown for: 4 V (circles), 5 V (squares), 6 V (triangles up) and 7 V (triangles down) with full markers in shades of blue and 8 V (circle), 9 V (squares), 10 V (triangles up) and 11 V (rhombs) with empty markers in shades of red. Bulk voltages are with respect to source.

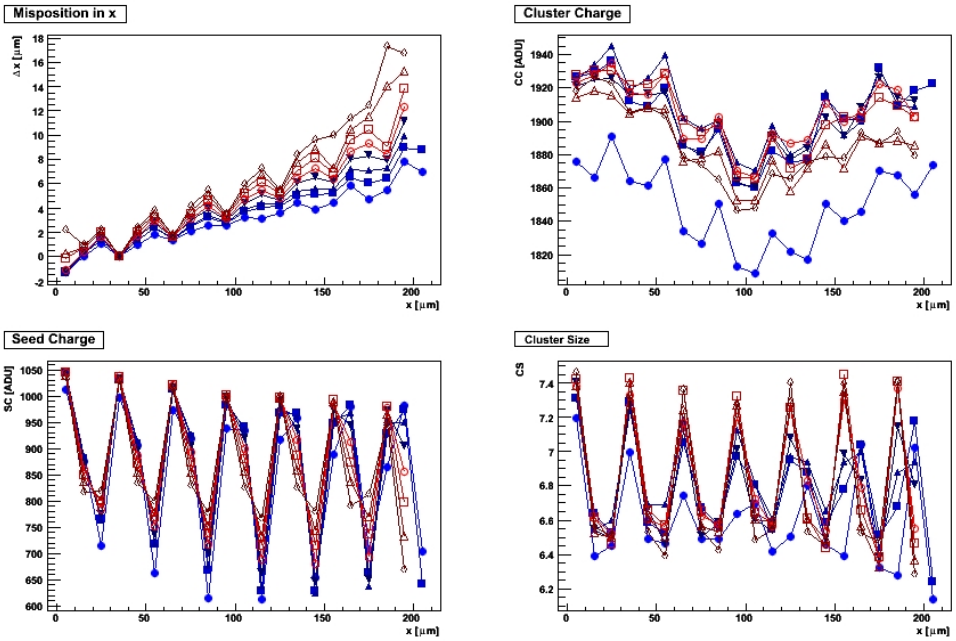

Figure 8: The graphs from right border show the mean of values with the same distance(of laser spot) from border as a function of laser spot position. A subset of data is shown for: 4 V (circles), 5 V (squares), 6 V (triangles up) and 7 V (triangles down) with full markers in shades of blue and 8 V (circle), 9 V (squares), 10 V (triangles up) and 11 V (rhombs) with empty markers in shades of red. Bulk voltages are with respect to source.

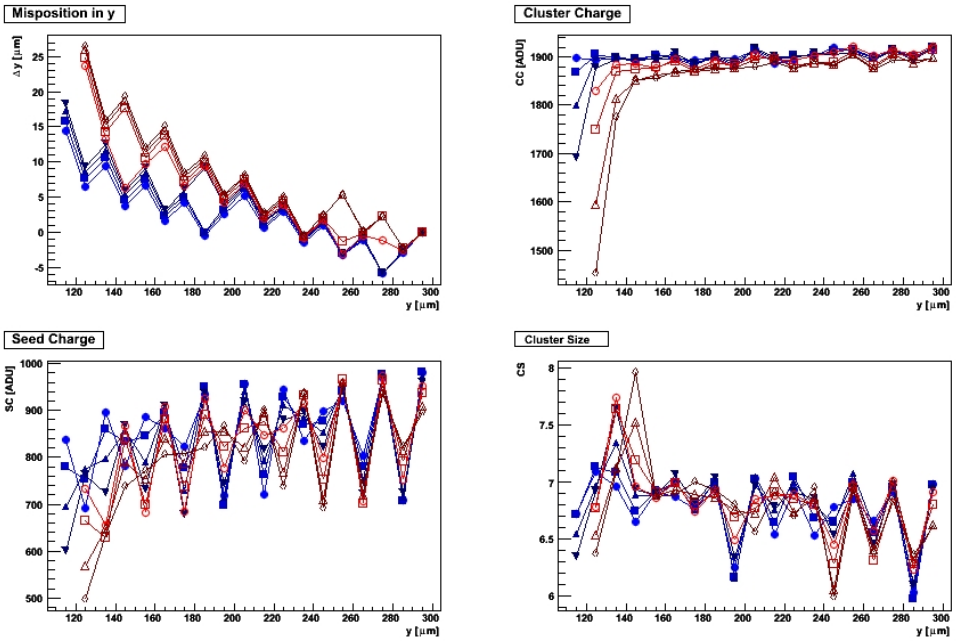

Figure 9: The graphs from top border show the mean of values with the same distance(of laser spot) from border as a function of laser spot position. A subset of data is shown for: 4 V (circles), 5 V (squares), 6 V (triangles up) and 7 V (triangles down) with full markers in shades of blue and 8 V (circle), 9 V (squares), 10 V (triangles up) and 11 V (rhombs) with empty markers in shades of red. Bulk voltages are with respect to source.

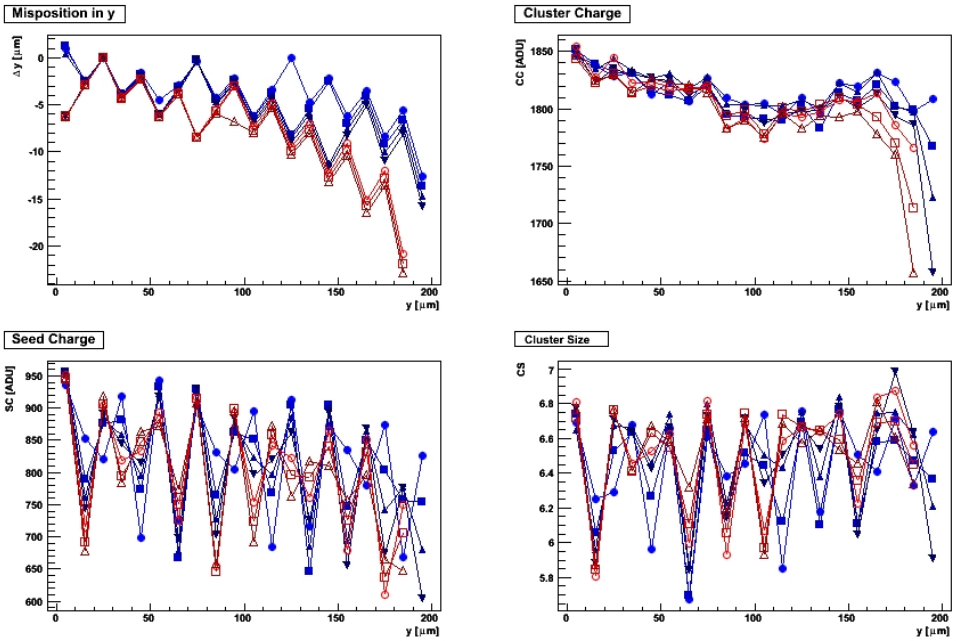

Figure 10: The graphs from bottom border show the mean of values with the same distance(of laser spot) from border as a function of laser spot position. A subset of data is shown for: 4 V (circles), 5 V (squares), 6 V (triangles up) and 7 V (triangles down) with full markers in shades of blue and 8 V (circle), 9 V (squares) and 10 V (triangles up) with empty markers in shades of red. Bulk voltages are with respect to source.

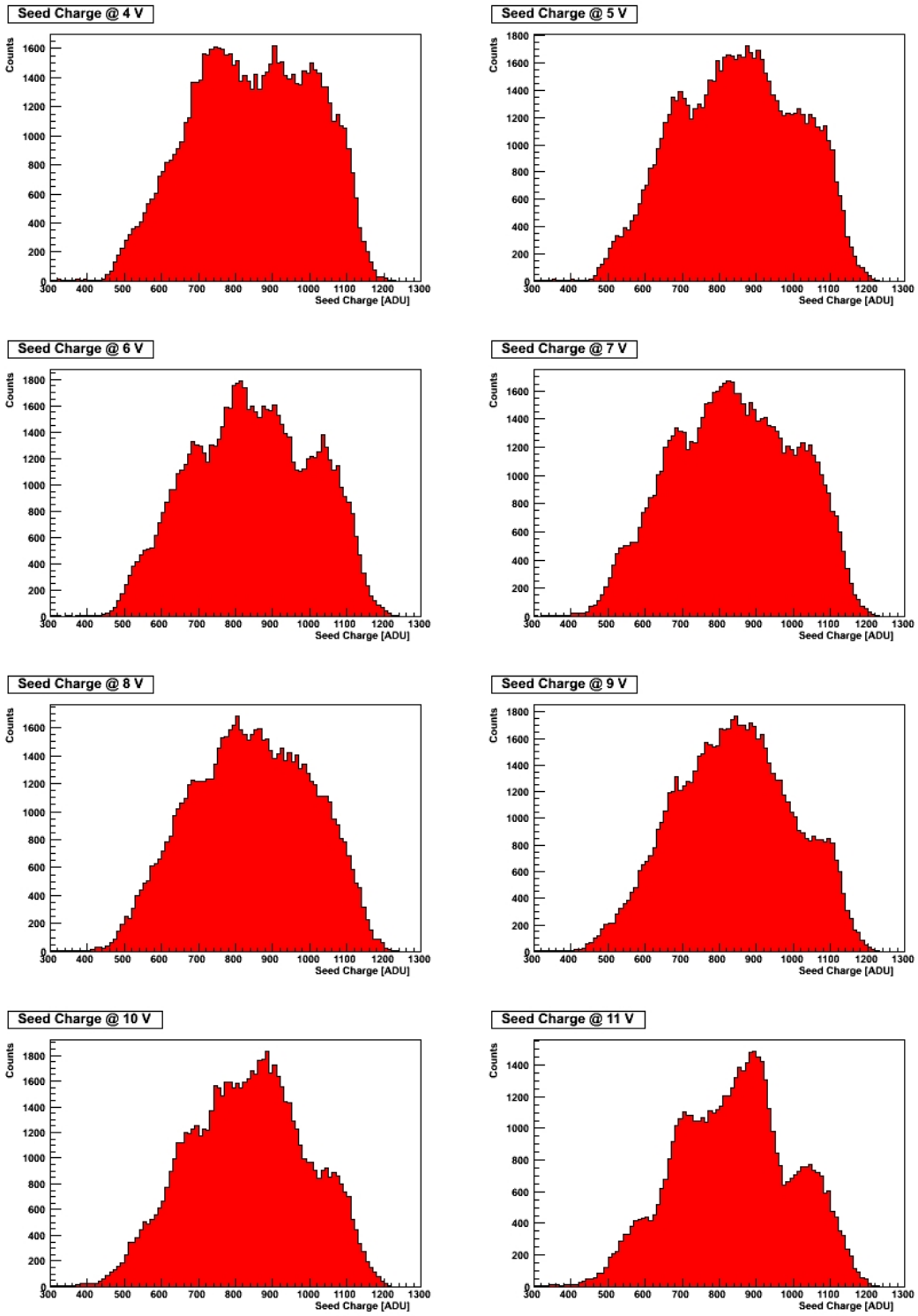

Figure 11: Seed charge histograms at different bulk voltages (with respect to source). The distributions are more influenced by large step of measurement than by bulk voltage.

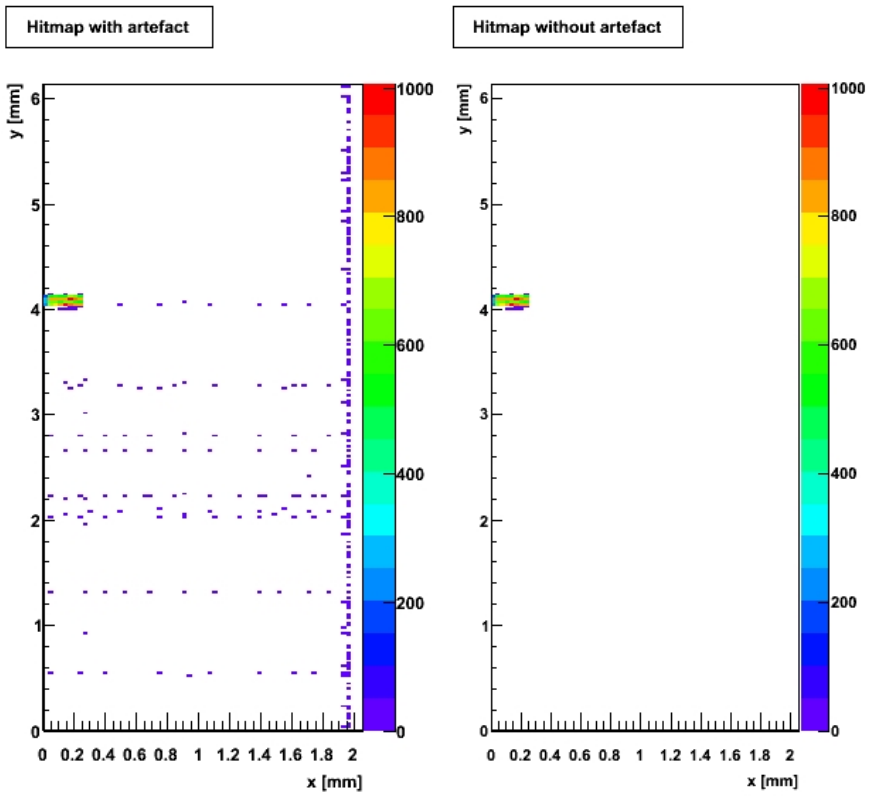

Figure 12: In the left map, there are single hits formed in the column and rows, they correspond to artefact of readout. In the right map is shown hits of the same run, artefact was removed.